PREDICTION OF WHEAT YIELD BY GENERAL LARGE AREA MODEL FOR ANNUAL CROPS AS DRIVEN BY REGIONAL CLIMATE MODEL AND OBSERVATIONAL DATA

By

Jemal A.

SUBMITTED IN PARTIAL FULFILLMENT OF THE
REQUIREMENTS FOR THE DEGREE OF
MASTER OF SCIENCE IN PHYSICS
AT
ADDIS ABABA UNIVERSITY
ADDIS ABABA, ETHIOPIA
JULY 2010

ADDIS ABABA UNIVERSITY
DEPARTMENT OF
PHYSICS

Supervisor: _____
Dr. Gizaw M.

Examiners: _____
Prof. A.V. Gholap

_____
Dr. Lemi Demeyu

ADDIS ABABA UNIVERSITY

Date: **JULY 2010**

Author: **Jemal A.**

Title: **Prediction of Wheat Yield by General Large Area Model for Annual Crops as driven by Regional Climate Model and Observational Data**

Department: **Physics**

Degree: **M.Sc.** Convocation: **JULY** Year: **2010**

Signature of Author

Table of Contents

List of Figures

Acknowledgements

Above all, I would like to thank the Almighty God for reasons too numerous to mention. “How numerous you have made your wondrous deeds, O Lord, our God! And in your plans for us there is none to equal you, should I wish to declare or tell them? They would be too many to recount”. Psalm 40:6

I would like to express my deep and sincere gratitude to my supervisor Dr. Gizaw Mengistu. His wide knowledge and his logical way of thinking have been of great value for me. His understanding and personal guidance have provided a good basis for the present thesis. I would like also to thank Dr. Sanai for her support in helping me understand and solve some of the problems that I have faced in this thesis.

My strongest thank is addressed to my amazing Family and to my wonderful Friends. They are my hero. If it were with out thier tremendous encouragement, support and patience through out my life, I could not have reached this stage.

I also want to thank Central Statistical Agency (CSA) of Ethiopia and Ethiopian Metrological Society for providing data that is used for this thesis work.

Abstract

A new process based crop model, the general large area model (GLAM) for annual crops and a Regional Climate Model (RegCM3) have been used for this study to predict the wheat yield in Southern nations, nationalities and people's region (SNNPR) of Ethiopia. This study aims to demonstrate how RegCM3 and GLAM could be used to forecast wheat yield. RegCM3 is used to predict precipitation, maximum temperature, minimum temperature and solar radiation over SNNPR. These variables are used in GLAM as inputs for yield forcast. All the internal consistency checks that are used to ensure the performance of the crop model prove that GLAM performs magnificently. The observed and the simulated yield exhibit a high correlation on the central part of the study area. However, GLAM yield has a negative bias which is found to be related with water stress. The water stress is confirmed from RegCM3 precipitation forcast which has a negative bias with respect to observed precipitation from Central Research Unit (CRU). As a result of this low correlation of observed and simulated yield has been detected in the North-east and South-west part. The model can be easily extended to any annual crop for the investigation of the impacts of climate variability (or change) on crop yield over large areas.

Chapter 1

Introduction

During the recent decade, the issues of climate variability and climate change have been at the center of many scientific studies. Global climate variability and change caused by natural processes as well as anthropogenic factors, are major and important environmental issues that will affect the world at the beginning of the 21^{st} century. The earth's climate has exhibited marked natural variations and changes, with time scales varying from many millions of years down to a few years. Over periods of 1 or 2 years, fluctuations in global surface temperatures of a few tenths of a degree have been recorded. Some of these are related to the El Nino-Southern Oscillation(ENSO) phenomenon; major volcanic eruptions have also had some impacts. The concentration of green house gases in the atmosphere continues to increase. This is largely due to human activities, mostly fossil fuel use, land use change, and agriculture. In some regions, there is also an increase in the concentration of aerosols, which has an opposite effect on the radiative balances and tend to cool the atmosphere. About 64% of the warming effect due to greenhouse gas increase during the last 200 years, is caused by carbondioxide. These changes in concentration of greenhouse gases and aerosols are projected to lead to regional and global changes in temperature, precipitation and other climate variables. This can ultimately result in global changes in soil moisture, an increase in global mean sea level, and prospects for more severe extreme high-temperature events, floods and droughts in many locations.

Global climate change will affect all economic sectors to some degree, but the agricultural

sector is perhaps the most sensitive and vulnerable. World agriculture, whether in developing or developed countries, remains very dependent on climate resources (Downing, 1996). The impact of climate variability on agricultural production is important at local, regional, national, as well as global scales. Crop yields are affected by variations in climatic factors such as air temperature and precipitation, and the frequency and severity of extreme events like droughts, floods, hurricanes, windstorms, and hail.

Recent research has focused on assessments of the potential impacts of climate change on agriculture at different scales. For example, regional and global estimates of potential climate change on agricultural production were conducted by Harrison et al. (1995), Wolf and Van Diepen (1995). The effects of global climate change and possible adaptation measures have been described by Easterling (1996), Smith (1997). Also several national assessments have been conducted by Rosenzweig et al. (1995), Peiris et al. (1996).

Weather and climate are key determinants of the productivity of crops grown in many regions of the world. Forcasts of crop production for the coming season require accurate seasonal forcastng. The development of crop simulation models and numerical weather prediction models present an opportunity to combine these models into a single crop and weather forcasting system. A successful forcasting crop yield could then support agricultural planning and give government bodies and aid agencies time to respond to impending shortages. On longer time scales such process based forcasting has the potential to provide skillfull forcasts for possible future climates where empirical methods would not necessarily be expected to perform well.

Ethiopia's economy is highly agricultural dependent, with more than 80% of the countries population bases thier life on agriculture. Further more it is the most vulunerable to weather and potential climate change. Hence weather variations pose a threat to food security. This needs reliable seasonal prediction in both current and future climates. Based on this climate predictions it is possible to assess what the crop yield will be at the end of the season.

1.1 Problem statement

The Ethiopian economy is based on subsistence agriculture, which accounts for more than half of the gross domestic product (GDP), 90% of exports and 80% of total employment. Ethiopia has great agricultural potential because of its vast areas of fertile land, diverse climate, generally adequate rainfall, and large labor pool. Despite this potential, however, Ethiopian agriculture has remained underdeveloped. Because of drought, which has repeatedly affected the country since the early 1970s, a poor economic base (low productivity, weak infrastructure, and low level of technology), and over population, the agricultural sector has performed poorly.

Ethiopian agriculture is based on small-scale peasant farmers. The production of its food and agricultural exports depends on them. So failure on the agricultural production means a lot for this country. Almost all farmers depends on rainfed agriculture with limited use of irrigation. It is highly dependent on both the quantity and timing of the seasonal rainfall. The agricultural sector suffers from frequent periods of drought, pest infestation and technologically limited farming practices.

Ingige, (2000) indicated that drought-prone tropical regions are characterized by a high variability of seasonal and annual rainfall across time and space. The Ethiopian climate has large interannual variability which can cause a severe drought and famine. For example the drought in 1970's causes 40,000 to 80,000 Ethiopians to be killed and so many died by 1980's drought.

So, this is a huge problem that the country faces for different times in the past. Finding the cause of this tremendaous obstacle which make the country poor and providing a solution for it could help the country to move one step in the forward direction.

1.2 Significance and objective of the study

Crop monitoring and forecasting is related to food security as one of the priority of policy strategy plan of Ethiopia. The development of the agricultural sector has been important to reduce poverty in rural communities, achieve food security and foster equitable and sustainable economic growth.

So far forcasting crop yields for climate projection in Ethiopia has not been practiced. One reason for this could be lack of crop models and how to use them for our purpose. So the need for forcasting wheat (crop) yields has good prospects for early warning of drought and famine, which occur so often in Ethiopia.

Solution for drought, in Ethiopia, successful development of productive capability for the study area seasonal yield anomalies is beneficial to planners and policy makers in making more constructive socioeconomic decisions, particularly with regards to food and agriculture.

In Ethiopia, it is important for determining import-export policies, government aid for farmers, taking care for food shortage, and allocation of subsidies for regional agricultural programs. By using the crop yield model, forecasts can be made at least many years before harvest, which would allow food security stakeholders enough time to secure crop imports in case of a deficit.

Chapter 2

Study area description

2.1 SNNPR

The Southern Nations, Nationalities and Peoples Region (SNNPR) is located in the southern and south-western part of Ethiopia. It roughly lies between 4.43-8.58 North latitude and 34.88-39.14 East longitude. It has common borders with Kenya in the South, the republic of Sudan in the South West, the state of Gambella peoples' in the North West and the state of Oromia in the North and East. Based on the data from the central statistical agency of Ethiopia (CSA) published in 2005, the SNNPR has an estimated total population of 14,901,990 consisting of 7,408,993 men, and 7,492,997 women. 13,625,000 or 91.4% of the population is estimated to be rural inhabitants, while 1,277,000 or 8.57% are estimated to be urban; this makes the SNNPR Ethiopia's most rural region. With an estimated area of 112,343 square kilometers, this region has an estimated density of 132.65 people per square kilometer. The region largely practices rainfed agriculture. Hence, unfavourable rainfall condition exposed the region to frequent drought and relief aid. About 56% of the total area of the state is found below 1500 meters elevation which is catagorized largely as hottest low land ("kolla"). The rest 44% is found in the temperate climatic zone.

Based on the availability of the yield data taken from the statistical agency for the study years, this study has covered the following regions:

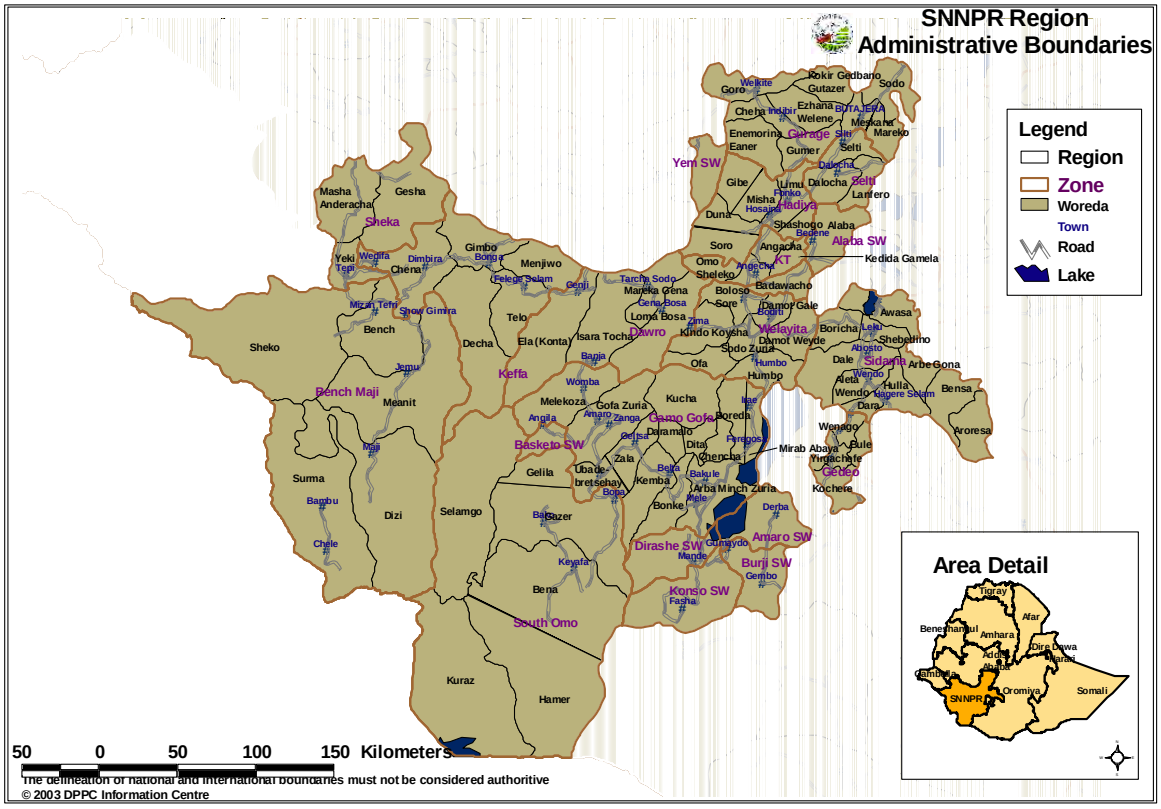

Figure 2.1: Map of current administrative zones and special weredas of SNNPR .

1. Gurage and Siltie ;
2. Alaba, Kembata, Tempbaro ;
3. Shekicho and Keficho ;
4. Hadia ;
5. North Omo (Gamo Gofa, Wolita, Dawro, Basketo, Konta) ;
6. Yem ;
7. Burji ; and
8. Amaro .

2.1.1 Rainfall

The amount, duration and intensity of rainfall in the region vary considerably. It generally decreases from west and northwest to south-eastwards. The main dry season is shorter in southern Ethiopia; conversely the main rainy season is larger in south west and in south. The past three decades rainfall data show that the mean annual rainfall of the region was ranging from the lowest about 400 mm in the extreme south of Debub Omo Zone to over 2200 mm in the west in Sheka and Kaffa zones. The lowest is experienced in parts of Debub Omo Zone such as Selamago, Benatsemay, Kuraz and Hamer Woredas, and in Bench Maji Zone such as Surma, Bero and Maji woredas. On the other hand highest values are recorded in Masha Woreda of Sheka Zone. Generally, in the western part of the region the rain occurs all the year round while it is bimodal in the eastern and southern part of the region.

Relying on the reliability of rainfall for crop production and duration of growing periods, the three seasonal pattern of rainfall in the region are Bega (December - February) which provides rain for limited part of the region, Belg (little rain season, March to April). The amount of rainfall received in Belg is relatively lower than the kiremt rainfall that occurrs in June, July, and August. However, in each of the seasons the rain may begin earlier/later and lasts before the usual time. This has impact on growing period and reliability of rainfall.

2.1.2 Temperature

The degree and intensity of temperature determines the rate of evapotranspiration, soil moisture content and the humidity of the atmosphere. The mean annual temperature of the region varies from less than 10^oC in the extreme highlands to the eastern parts of Sidama highlands to over 27^oC in the lowlands to the south in the Omo rate plain (Debub Omo Zone).

However, temperatures are generally high in the region with little variations among seasons. The mean annual maximum temperature of the region ranges from 31^oC in Debub Omo zone to about 21.7^oC in Gurage zone. On the other hand the mean annual minimum temperature roughly varies from 11^oC in the high lands of Siltie zone to about 18.4^oC in the lowland of Gamogofa and Dawro Zones and Konso Special Woreda.

Chapter 3

Factors affecting crop yield and wheat crop in Ethiopia

3.1 Climate and crop relation, and other yield determing factors

A crop is the annual or season's yield of any plant that is grown in a significant quantities to be harvested as food, as livestock fodder, fuel, or for any other economic purpose. Plant growth and development are primarily governed by the environmental conditions of the soil and climate. The success or failure of farming is intimately related to the prevailing weather conditions. Weather assumes significance in nearly every phase of agricultural activity from the preparatory tillage to harvesting and storage. As weather is the single major limiting factor in crop production successful farming calls for appropriate decisions in light of weather conditions in the time of sowing, transplanting, scheduling of irrigation, timing of fertilliser application, use of pesticides, etc.

3.1.1 Rainfall and crop

Both weather and climate affect virtually every aspect of agriculture, from the production of crops and livestock to the transportation of agricultural products to market. Agricultural crop production is likely to be affected by both climate change and the associated increase in atmospheric CO_2. The projected changes in temperature and precipitation have the potential to affect crop yields either positively or negatively; elevated CO_2 levels increase plant photosynthesis and thus crop yields. Changes in climatic conditions are also likely to alter livestock performance and growth, grazing availability, irrigation water supply and demand, pest populations, and incidence of extreme events (floods, droughts, hail, etc.).

The primary source of water for agricultural production for most of the world is rainfall. Three main characteristics of rainfall are its amount, frequency and intensity, the values of which vary from place to place, day to day, month to month and also year to year. Precise knowledge of these three main characteristics is essential for planning its full utilization. Changes in precipitation and increased evapotranspiration could lead to water shortages in some regions of the world. Access to water is a key factor in ensuring food security. Agriculture, which accounts for almost 70% of global water use, will be severely impacted by water stress (FAO 2005a). Precipitation changes will also affect soil moisture. Precipitation, especially rain, has a dramatic effect on agriculture. All plants need at least some water to survive, therefore rain (being the most effective means of watering) is important. A regular rain pattern is usually vital to healthy plants, too much or too little rainfall can be harmful, even devastating to crops. Drought can kill crops and increase erosion, while overly wet weather can cause harmful fungus growth.

When water supply does not meet crop water requirements, actual evapotranspiration (ET_a) will fall below maximum evapotranspiration (ET_m) or the reverse. Under this condition, water stress will develop in the plant which will adversely affect crop growth and ultimately crop yield. The effect of water stress on growth and yield depends on the crop

species and the variety on the one hand and the magnitude and the time of occurrence of water deficit on the other. The effect of the magnitude and the timing of water deficit on crop growth and yield is of major importance in scheduling available but limited water supply over growing periods of the crops and in determining the priority of water supply amongst crops during the growing season.

Crops vary in their growth and yield response to water deficit. When crop water requirements are fully met by available supply ($ET_a = ET_m$), the amount of total dry matter and yield produced per unit of water (kg/m^3) varies with crop. This can be expressed as the water utilization efficiency in kg/m^3 for total dry matter (E_m) and harvested yield (E_y).

Crops have different growth rates and crop water requirements; also the portion of the total dry matter that is harvested as yield varies with the crop. When actual evapotranspiration equals maximum evapotranspiration, these differences in growth and yield result in differences in dry matter and harvested yield. For example, dry matter for groundnut is about 1.6 and for maize about 2.5; with harvest index (HI) for groundnut (unshelled) equal to 0.35 and for maize 0.40 and taking into account the moisture percentage of the harvested part specific to the crop, the value of harvested yield for groundnut is about 0.65 and for maize about 1.15. However, as harvested yield also depends on the harvest index and the moisture percentage of the harvested part, a high dry matter does not always lead to a high harvested yield.

When water supply does not meet crop water requirements, or $ET_a > ET_m$, crops vary in their response to water deficits. In some crops there is an increase in water utilization efficiency whereas for other crops harvested yield decreases with increase in water deficit. For example, with a water deficit spread equally over the total growing season, harvested yield will decrease for maize and increase somewhat for sorghum under similar climatic conditions. Although yield per unit area (kg/ha) for both crops will be lower when water supply is limited, the yield reduction will be greater in the case of maize.

When water deficit occurs during a particular part of the total growing period of a crop, the yield response to water deficit can vary greatly depending on how sensitive the crop is at that growth period. In general, crops are more sensitive to water deficit during emergence, flowering and early yield formation than they are during early (vegetative, after establishment) and late growth (ripening) periods .

3.1.2 Temperature and crop

Temperature is central to how climate influences the growth and yield of crops. The rate of many growth and development processes of crop plants is controlled by air or soil temperature. Over the last decade or so, the interests of the scientific community in the response of crops to temperature has been renewed as the evidence of a warming of global mean temperatures due to human activities becomes more persuasive.

Many studies have investigated how the warmer temperatures and elevated atmospheric CO_2 concentrations expected under climate change scenarios affect crop plants (reviewed in Morison and Lawlor, 1999). In general, an increase in mean seasonal temperature of 2–4 ^oC reduces the yield of annual crops of determinate growth habit, such as wheat (Triticum aestivum L.) (Wheeler et al., 1996a; Batts et al., 1997), grown in well-watered conditions. Much of this decline in yield is due to shorter crop durations at these warmer temperatures. Nevertheless, this decline is expected to be countered by the enhancement of the rate of photosynthesis under future conditions of elevated atmospheric CO_2 concentrations. For example, a decline of wheat yield due to mean seasonal temperatures of 4.5^oC (Goudriaan and Unsworth, 1990) and 1.8^0C (Wheeler et al., 1996a) warmer were entirely offset by a doubling of atmospheric CO_2 concentration. In addition, reductions in the yield of determinate crops due to shorter crop durations could be countered by changing to a cultivar which has a longer crop duration in future climates through different sensitivities to temperature and/or photoperiod. Thus, the combined impact of warmer mean seasonal temperatures of 2–4 ^oC and elevated atmospheric CO_2 concentrations of

about 700 ppm at the end of the 21st century on the yield of current cultivars of annual crops grown in environments with sufficient water may not be great.

The effects of differences in mean seasonal temperature on crops are better understood than those of the fluctuating temperatures of many natural environments. For example, the rate of many development processes is a positive linear function of temperature between a base temperature (at and below which the rate of a particular process is zero) and an optimum temperature, and a negative linear function of temperature between this optimum and a ceiling temperature. Many development processes of crop plants conform to these relationships. For example, the rate of seed germination (Garcia-Huidobro et al., 1982), the rate of flowering of photoperiod insensitive crop genotypes and photoperiod sensitive genotypes continuously grown in inductive photoperiods (Hadley et al., 1983), and the rate of grain filling of cereals (Slafer and Rawson, 1994; Wheeler et al., 1996b). Thus, the response of these processes to changes in mean seasonal temperature can be easily quantified provided that the base or optimum temperatures are not transgressed for substantial periods of time.

Nevertheless, the effects of variability in temperature on crops may also be important. First, the effects of weather variables on crops are often non-linear because of the ways in which many crop processes respond to environment. Second, fluctuations of extreme temperatures may affect the survival of crop plants or plant organs. The lethal temperatures for many growth and development processes of wheat have been clearly defined (Porter and Gawith, 1999). Under such extreme conditions, crop plants are loosely defined as under temperature or thermal stress. Recognition of the effects of temperature stress implies a comparison with plant performance under optimal conditions of temperature. Accordingly, resistance of crop plants to temperature stress has been defined as the maintenance of economic value where the crop is exposed to temperature stress. Such definition does not consider the mechanisms responsible for temperature stress. Alternatively, stress temperatures are more simply defined as those hotter (or colder) than a

specific temperature. For example, Srinivasan et al. (1996) defined hot temperatures as those >30^{o}C, and then identified regions where tolerance to hot temperatures would be a useful attribute for both vegetative growth and flowering of four grain legumes. Regardless of a precise definition, it is clear that the impact of temperature variability on crops is likely to include tolerance of crops to episodes of stress temperatures.

3.1.3 Soil types

Water is essential in the plant environment for a number of reasons. Water transports minerals through the soil to the roots where they are absorbed by the plant. Water is also the principal medium for the chemical and biochemical processes that support plant metabolism. Under pressure within plant cells, water provides physical support for plants. It also acts as a solvent for dissolved sugars and minerals transported throughout the plant. In addition, evaporation within intercellular spaces provides the cooling mechanism that allows plants to maintain the favorable temperatures necessary for metabolic processes. Water is transported throughout plants almost continuously. There is a constant movement of water from the soil to the roots, from the roots into the various parts of the plant, then into the leaves where it is released into the atmosphere as water vapor through the stomata (small openings in the leaf surfaces). This process is called transpiration. Combined with evaporation from the soil and wet plant surfaces the total water loss to the atmosphere is called evapotranspiration.

A soil is made up of various amounts of sand, silt, clay, and organic material, as well as pore space. The pore space is filled with either air or water. The ideal mixture is 50% soil, 25% water, and 25% air. Under these conditions the turf expends a minimal amount of energy to uptake water and nutrients. The size, shape, and arrangement of the soil particles and the associated voids (pores) determine the ability of a soil to retain water. It is important to realize that large pores in the soil can conduct more water more rapidly than fine pores. In addition, removing water from large pores is easier and requires less energy

than removing water from smaller pores. The role of soil in the soil-plant-atmosphere continuum is unique. It has been demonstrated that soil is not essential for plant growth and indeed plants can be grown hydroponically (in a liquid culture). However, usually plants are grown in the soil and soil properties directly affect the availability of water and nutrients to plants. Soil water affects plant growth directly through its controlling effect on plant water status and indirectly through its effect on aeration, temperature, and nutrient transport, uptake and transformation.

The soil system is composed of three major components: solid particles (minerals and organic matter), water with various dissolved chemicals, and air. The percentage of these components varies greatly with soil texture and structure. An active root system requires a delicate balance between the three soil components; but the balance between the liquid and gas phases is most critical, since it regulates root activity and plant growth process. The amount of soil water is usually measured in terms of water content as percentage by volume or mass, or as soil water potential. Water content does not necessarily describe the availability of the water to the plants, nor indicates, how the water moves within the soil profile. The only information provided by water content is the relative amount of water in the soil.

Water-holding capacity is controlled primarily by soil texture and organic matter. Soils with smaller particles (silt and clay) have a larger surface area than those with larger sand particles, and a large surface area allows a soil to hold more water. In other words, a soil with a high percentage of silt and clay particles, which describes fine soil, has a higher water-holding capacity. The table illustrates water-holding-capacity differences as influenced by texture. Organic matter percentage also influences water-holding capacity. As the percentage increases, the water-holding capacity increases because of the affinity organic matter has for water.

3.1.4 Planting date

Proper planting practices are the first step to overcoming yield limitations the environment can put on a crop. Planting date is one of the most important and least expensive ways to impact crop yield.

Planting date dictates to a large degree how many tillers a plant will make, how tall the plants will get, and the potential impact of certain insects and diseases on the crop. It also determines the size of the root system, which in turn determines how much stored water the plant can utilize. Optimum planting dates vary from region to region, and depend on local environmental conditions. In addition, proper sowing time being one of the important factors for achieving optimum yield of wheat in dryland regions. Previous researches showed that optimum sowing gave higher grain yield than later sowing. While too early sowing produces weak plants with poor root system. Moreover, the temperature being above the optimum during too early sowing deals to irregular germination. Overall, research has shown a small yield loss with very early planting dates and a larger yield loss with late planting dates. The later the planting date, the more rapid the yield penalty accelerates. Planting dates can be greatly impacted by weather. Yield loss in delayed plantings can be attributed to decreased pod numbers. Later planted wheat does not develop roots deep enough to fully utilize deep soil moisture. The lack of root development in late planted wheat may make it susceptible to drought and winter injury (Winter and Musick, 1993). Earlier planted wheat is more vulnerable to insects and viral infection.

3.2 Wheat production in Ethiopia

Agriculture is a dominant sector in Ethiopia. Crops are the major agricultural commodities on which Ethiopians depend for thier daily food. Compared to other countries Ethiopia is an outstanding wheat producer in Africa. The country's altitude plays an

important role in the distribution of wheat production, and it is thought to influence rainfall, temperature and disease. Wheat grows at a range between 6 and 16 degree north and 35 and 42 degree East. From 1800 to 2800 meters above sea level. In Ethiopia, wheat is cultivated as a rainfed crop by small farmers in the highland regions of the country. The bulk of wheat crop is grown during the longer rainy season (meher) which usually starts in June. The meher crop season is the main season and produces 90-95% of the nations total cereals output. During the short rainy season (Belg) starting in March (which covers 5-10% output), growing wheat implies harvesting during meher, which results in high grain moisture. The type of soil for cultivation of the crop varies from region to region and it can usually grow in black and clay types of soil. Wheat crops are typically sown in June or July and harvested in November or December. Wheat is the fifth most important cereal crop in Ethiopia. In area of production, it ranks 5^{th} after teff, maize, barley and sorghum and in total grain production, it ranks 4^{th} after maize, teff and sorghum. In productivity, wheat ranks 2^{nd} to maize. It accounts for more than 15% of the total cereal output. It is an important crop commodity, which could contribute a major part in achieving the country's agricultural policy objective of food grain self-sufficiency. Ethiopia is the largest wheat producer in Sub-Saharan Africa with about 0.75 million ha of durum and bread wheat. Wheat is one of the major cereal crops grown in the Ethiopian highlands. The most suitable areas for wheat production, however, fall between 1900 and 2700 m. In the highlands, rainfall distribution is bimodal and ranges between 600 and 2000 mm/annum. The rainy season is divided into the short rains (Belg) falling from February to April and the main rains (Meher) falling from June to September. At present, wheat is produced solely under rainfed conditions. Currently, about 60% of the wheat area is covered by durum and 40% by bread wheat. The estimate for 1967 consisted of about 15% for bread wheat and 85% for durum.

Nastasi (1964) reported that Gojam, Harar, Shewa, Tigray, and Wollo were major wheat producing areas. At present, 75.5% of the total wheat production comes from Arsi, Bale,

and Shewa regions. Forty-six percent of the 1.3 million ha classified as highly suitable for wheat production is found in Arsi and Shewa. The regions identified as highly suitable for wheat production include Arsi, S. Shewa, W. Shewa, N. Shewa, Ilubabor, W. Harerge, Sidamo, Tigray, N. Gonder, Bale and Gojam.

Figure 3.1: Wheat production distribution in Ethiopia .

Altitude plays an important role in the distribution of wheat production through its influence on rainfall, temperature, diseases and pests. In addition to overall productivity, elevation influences plant characters such as caryopsis structure and pigmentation of glumes and awns. It has been reported that wheat grown at higher altitudes (2200-2700 m) has vitreous kernels and deeper pigmentation of the spikes, which may be melanic or anthocyanic, while wheat grown at lower altitudes (1800- 2000 m) exhibits yellow-berry kernel symptoms and a complete absence of pigmentation of the glumes and awns. Elevations between 2000 and 2200 m seem to be transitional zones, where mixed symptoms of both pigmentation and yellow-berry can be observed.

Soil types and moisture regimes of the wheat producing regions vary from area to area. In Arsi, Bale, and Shewa regions, where about 85% of the bread wheat is presently grown, the soil moisture and disease conditions in the 1900-2300 m altitude zone are favorable

for the production of early and intermediate maturing varieties of bread wheat area while the remaining 75% falls in the 2300-2700 m altitude zone. The soil types used for wheat production vary from well-drained fertile soils to waterlogged heavy Vertisols.

A recently held workshop on research priority setting concluded that bread wheat is a number one priority among cereals. Currently, Ethiopia is only 65% self sufficient in wheat. By the year 2000, the national wheat requirement is estimated to be 2.2 million tonnes, thus indicating the need to increase the current national wheat yield level from 1.3 tonnes/ha to 2.2 tonnes/ha. Therefore, Ethiopia needs to increase wheat production and productivity in order to meet one of its national agricultural policy objectives of food self-sufficiency. Over the last ten years, the trend in wheat production showed more or less no increase during the first seven years and showed a slight increase during the last three years both in area and total grain yield. An increase in production during the latter years may be attributed to improved and better-adapted varieties, improved production practices, increased local demand and better market prices.

Chapter 4

Method: formulation of crop yield hindcasts

4.1 Regional Climate Model (RegCM3)

Climate varies across a wide range of temporal and spatial scales. Yet, climate modeling has long been approached using global models that can model only the broad scales of atmospheric circulations and their interaction with convective cells, land, ocean circulation, and other environmental variables. An alternative to global modeling is regional climate modeling. As the name implies, a regional climate model (RegCM) does not attempt to simulate the entire globe but only a small portion. The inherent physics and mathematics behind General Circulation Model (GCMs) still applies to the RegCM, but by downscaling the climate model we can understand trends of synoptic and mesoscale weather events under climate change. RegCMs have an average spatial extent that varies from 100 km^2 to 25 km^2. Regional climate models are typically coupled with GCMs to incorporate initial meteorological and environmental boundary conditions within the RegCM. RegCMs can be used to provide information on finer scale climate responses. So, seasonal weather prediction can now be routinely carried out using Regional climate model (RegCM). RegCM provides probabilistic predictions of the seasonal mean climate. It also produces daily time series of the evolution of the weather and thus provide information on the statistics of the weather during the season. These daily time series can be used to drive process

based applications models such as a crop model; however, some spatial downscaling of the data may be required. As an alternative, the mean forecasts can then be used as inputs to a weather generator that produces a time series consistent with both the probabilistic climate scenarios and locally observed weather patterns. This approach can have the further advantage of matching the scale of the weather input to that of the application. Because of interactions between the weather and crop are important, in particular at critical phenological stages (Wheeler et al. 2000), it is weather rather than climate prediction that is needed for crop modeling applications. Hence, although the prediction of weather at seasonal lead times is not possible deterministically, where the term seasonal weather forecasting is used in this paper it refers to the estimation of daily weather values months in advance. Forecasts of climate cannot form the input to a crop model because the temporal resolution is too low, and it is for this reason that the term climate forecast is avoided. The weather data used as input to the crop model in this study come from the regional climate modeling (RegCM3). Maximum and minimum temperature, solar radiation and rainfall are the main climate variables which are used as an input in the forcasting system.

4.1.1 Model description

Atmospheric motions are governed by three fundamental physical principles: conservation of mass, conservation of momentum, and conservation of energy. The mathematical relations that express these laws may be derived by considering the budgets of mass, momentum, and energy for an infinitesimal control volume in the fluid. These conservation laws can be applied to a control volume of the atmosphere at a fixed location (Eulerian) or to a control volume of the atmosphere that is moving with the flow (Lagrangian).

4.1.2 The RegCM3 model horizontal and vertical grid

It is useful to first introduce the models grid configuration. The modeling system usually gets and analyzes its data on pressure surfaces, but these have to be interpolated to the models vertical coordinate before input to the model. The vertical coordinate is terrain-following (Fig. 4.1) meaning that the lower grid levels follow the terrain while the upper surface is flatter. Intermediate levels progressively flatten as the pressure decreases toward the top of the model. A dimensionless σ coordinate is used to define the model levels where p is the pressure, p_t is a specified constant top pressure, p_s is the surface pressure:

$$\sigma = \frac{(p - p_t)}{(p_s - p_t)} \tag{4.1.1}$$

It can be seen from Eq. (4.1.1) and Fig. 4.1 that σ is zero at the top and one at the surface, and each model level is defined by a value of σ. The model vertical resolution is defined by a list of values between zero and one that do not necessarily have to be evenly spaced. Commonly the resolution in the boundary layer is much finer than above, and the number of levels may vary upon the user demand.

The horizontal grid has an Arakawa-Lamb B-staggering of the velocity variables with respect to the scalar variables. This is shown in Fig. 4.2 where it can be seen that the scalars (T, q, p, etc.) are defined at the center of the grid box, while the eastward (u) and northward (v) velocity components are collocated at the corners. The center points of grid squares will be referred to as cross points, and the corner points are dot points. Hence horizontal velocity is defined at dot points. Data is input to the model, the preprocessors do the necessary interpolation to assure consistency with the grid.

All the above variables are defined in the middle of each model vertical layer, referred to as half-levels and represented by the dashed lines in Fig. 4.1. Vertical velocity is carried at the full levels (solid lines). In defining the sigma levels it is the full levels that are listed, including levels at $\sigma = 0$ and 1. The number of model layers is therefore always one less than the number of full sigma levels.

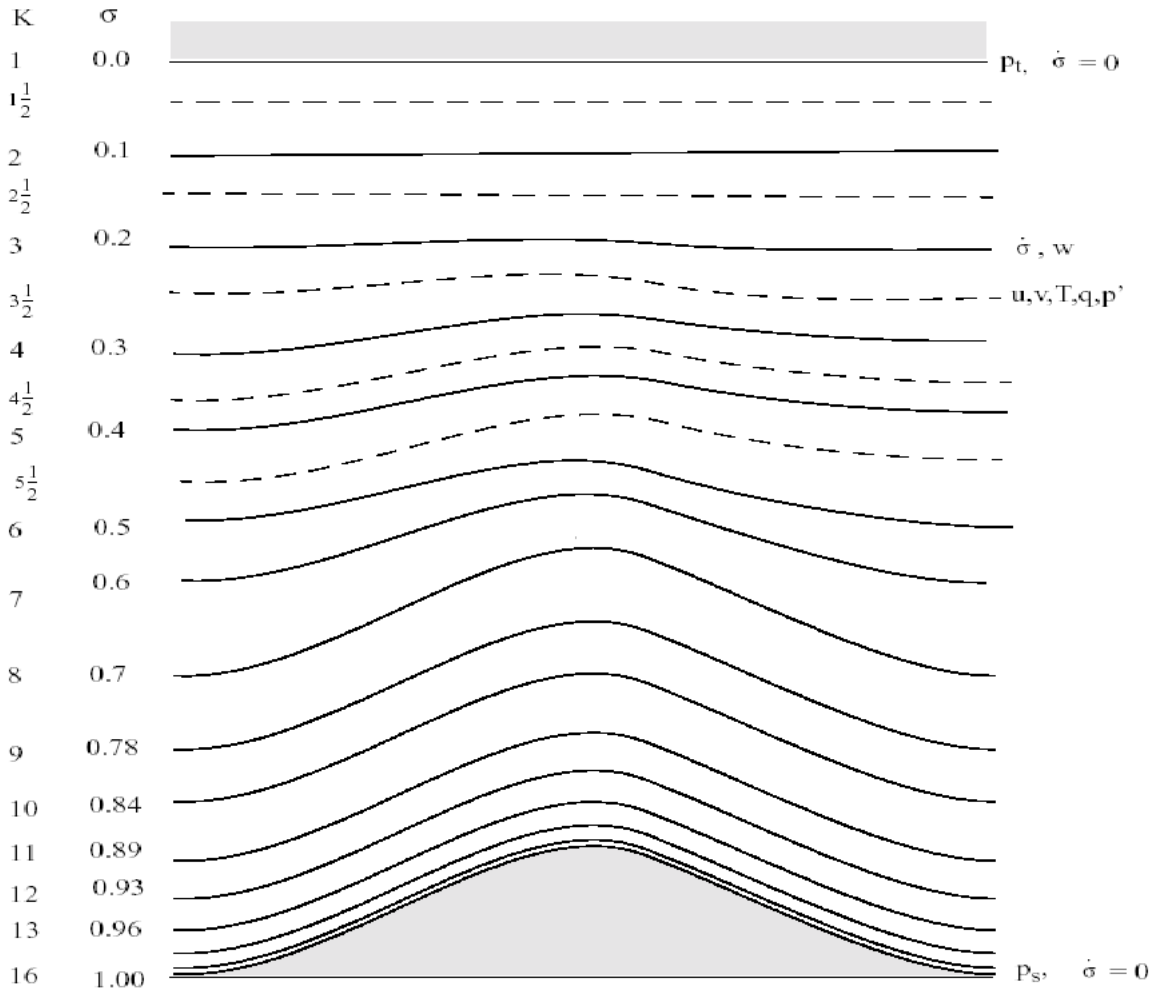

Figure 4.1: Schematic representation of the vertical structure of the model. This example is for 16 vertical layers. Dashed lines denote half-sigma levels, solid lines denote full-sigma levels. (Adapted from the PSU/NCAR Mesoscale Modeling System Tutorial Class Notes and Users Guide.) .

The finite differencing in the model is, of course, crucially dependent upon the grid staggering wherever gradients or averaging are represented.

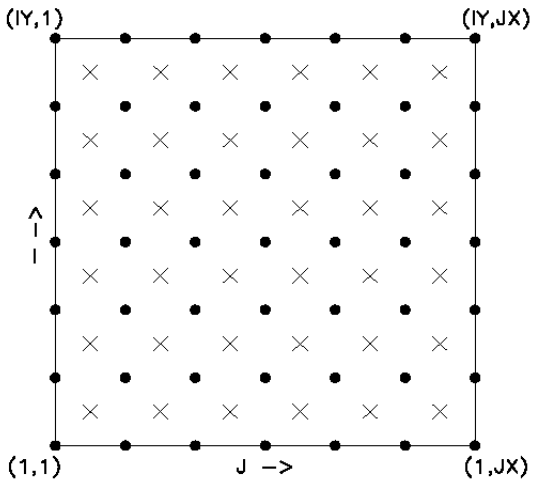

Figure 4.2: Schematic representation showing the horizontal Arakawa B-grid staggering of the dot and cross grid points. .

4.1.3 Model dynamics

Momentum equations

Newtons second law for motion relative to a rotating coordinate frame is given by

$$\frac{D\vec{U}}{Dt} = \frac{1}{M_a}[-F_{coriol} + (F_{cent} + F_{grav}) + F_{prgrad} + F_{others}] \tag{4.1.2}$$

where F_{coriol}, F_{cent}, F_{grav}, F_{prgrad} are corriolis force, centripetal force, gravitational force and pressure gradiant force respectively. This can be rewritten explicitely as

$$\frac{D\vec{U}}{Dt} = -\frac{1}{\rho}\nabla P_a - \nabla\phi + f\hat{k}X\vec{V} + f_{others} \tag{4.1.3}$$

Where the LHS can be expanded

$$\frac{D\vec{U}}{Dt} = \frac{\partial\vec{U}}{\partial t} + u\frac{\partial\vec{U}}{\partial x} + v\frac{\partial\vec{U}}{\partial y} + w\frac{\partial\vec{U}}{\partial z} \tag{4.1.4}$$

By equating the above two equations, we obtain

$$\frac{\partial u}{\partial t} = -u\frac{\partial u}{\partial x} - v\frac{\partial u}{\partial y} - w\frac{\partial u}{\partial z} - \frac{1}{\rho}\frac{\partial P}{\partial x} - fv + f_{others} \tag{4.1.5}$$

$$\frac{\partial v}{\partial t} = -u\frac{\partial v}{\partial x} - v\frac{\partial v}{\partial y} - w\frac{\partial v}{\partial z} - \frac{1}{\rho}\frac{\partial P}{\partial y} - fu + f_{others} \tag{4.1.6}$$

These momentum equations can be written using sigma coordinate system as

$$\frac{\partial p^\star u}{\partial t} = -m^2\left(\frac{\partial p^\star uu/m}{\partial x}+\frac{\partial p^\star vu/m}{\partial y}\right)-\frac{\partial p^\star u\dot{\sigma}}{\partial \sigma}-mp^\star\left[\frac{RT_v}{p^\star+p_t/\sigma}\frac{\partial p^\star}{\partial x}+\frac{\partial \phi}{\partial x}\right]+fp^\star v+F_H u+F_V u \tag{4.1.7}$$

$$\frac{\partial p^\star v}{\partial t} = -m^2\left(\frac{\partial p^\star uv/m}{\partial x}+\frac{\partial p^\star vv/m}{\partial y}\right)-\frac{\partial p^\star v\dot{\sigma}}{\partial \sigma}-mp^\star\left[\frac{RT_v}{p^\star+p_t/\sigma}\frac{\partial p^\star}{\partial y}+\frac{\partial \phi}{\partial y}\right]-fp^\star u+F_H v+F_V v \tag{4.1.8}$$

where u and v are the eastward and northward components of velocity, T_v is virtual temperature, ϕ is geopotential height, f is the coriolis parameter, R is the gas constant for dry air, m is the map scale factor for either the Polar Stereographic, Lambert Conformal, or Mercator map projections, $\dot{\sigma} = \frac{\partial \sigma}{\partial t}$, and F_H and F_V represent the effects of horizontal and vertical diffusion, and $p^\star = p_s - p_t$.

Continuity and vertical velocity equations

The continuity equations for air, individual gases, and aerosol particles, and the thermodynamic energy equation are fundamental equations in atmospheric models. Continuity equations are used to simulate changes in concentration or mixing ratio of a variable over time and take account of transport, external sources, and external sinks of the variable. Considering a unit volume (see fig. 4.3), the net rate of mass inflow through the sides equals the rate of accumulation of mass within a volume. The rate of inflow of mass through the left-hand face per unit area is

$$[\rho u - \frac{\partial}{\partial x}(\rho u)\frac{\delta x}{2}] \tag{4.1.9}$$

whereas the rate of outflow per unit area through the right-hand face is

$$[\rho u + \frac{\partial}{\partial x}(\rho u)\frac{\delta x}{2}] \tag{4.1.10}$$

Because the area of each of these faces is $\delta y \delta z$, the net rate of flow into the volume due to the x velocity component is

$$[\rho u - \frac{\partial}{\partial x}(\rho u)\frac{\delta x}{2}]\delta y \delta z - [\rho u + \frac{\partial}{\partial x}(\rho u)\frac{\delta x}{2}]\delta y \delta z \quad = -\frac{\partial}{\partial x}(\rho u)\delta x \delta y \delta z \tag{4.1.11}$$

Similar expressions obviously hold for the y and z directions. Thus, the net rate of mass

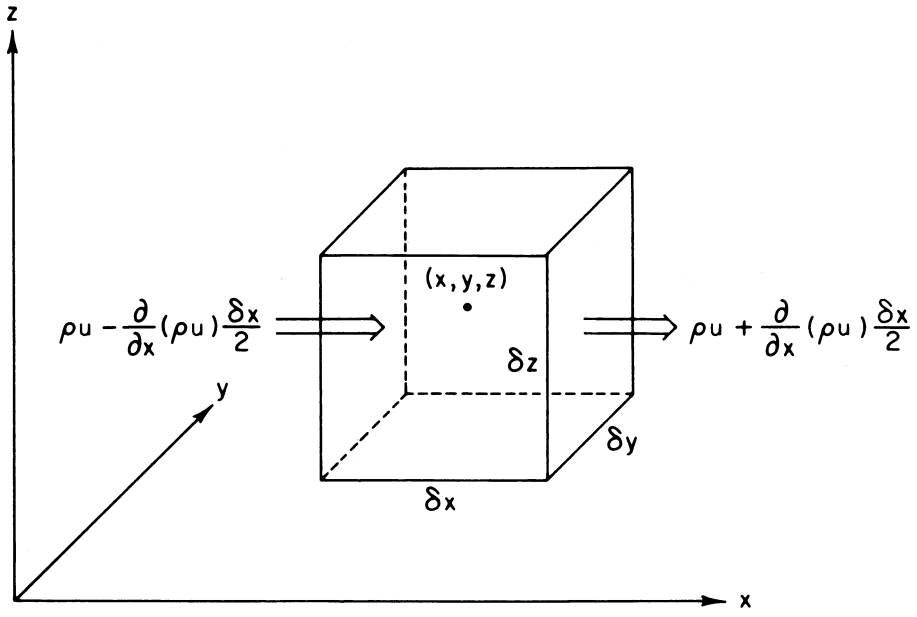

Figure 4.3: Mass inflow into a fixed (Eulerian) control volume due to motion parallel to the x axis.

inflow is

$$-[\frac{\partial}{\partial x}(\rho u) + \frac{\partial}{\partial y}(\rho v) + \frac{\partial}{\partial z}(\rho w)]\delta x \delta y \delta z \tag{4.1.12}$$

and the mass inflow per unit volume is just -$\nabla.(\rho U)$ where U=iu + jv + kw, which must equal the rate of mass increase per unit volume. Now the increase of mass per unit volume is just the local density change $\frac{\partial \rho}{\partial t}$. Therefore,

$$\frac{\partial \rho}{\partial t} + \nabla.(\rho U) = 0 \tag{4.1.13}$$

The continuity equation can be written in sigma coordinate system, as

$$\frac{\partial p^\star}{\partial t} = -m^2(\frac{\partial p^\star u/m}{\partial x} + \frac{\partial p^\star v/m}{\partial y}) - \frac{p^\star \dot{\sigma}}{\partial \sigma} \tag{4.1.14}$$

The vertical integral of Eq. (4.1.14) is used to compute the temporal variation of the surface pressure in the model,

$$\frac{\partial p^\star}{\partial t} = -m^2 \int_0^1 (\frac{\partial p^\star u/m)}{\partial x} + \frac{\partial p^\star v/m}{\partial y}) d\sigma \tag{4.1.15}$$

After calculation of the surface-pressure tendency $\frac{\partial p^\star}{\partial t}$, the vertical velocity in sigma coordinate ($\dot{\sigma}$) is computed at each level in the model from the vertical integral of Eq. (4.1.14)

$$\dot{\sigma} = -\frac{1}{p^\star} \int_0^\sigma [\frac{\partial p^\star}{\partial t} + m^2 (\frac{\partial p^\star u/m}{\partial x} + \frac{\partial p^\star v/m}{\partial y})] d\sigma^{'} \tag{4.1.16}$$

where $\sigma^{'}$ is a dummy variable of integration and $\dot{\sigma}(\sigma = 0)$=0.

Thermodynamic equation

The thermodynamic energy equation is used to predict changes in temperature with time and takes account of transport, external sources, and external sinks of energy. The 1^{st} law of thermodynamic is used to relate the change in temperature of a parcel of air to energy transfer between the parcel of air and the environment and work done by or on a parcel:

$$dQ = dU + dW \tag{4.1.17}$$

where dQ is called the diabatic heating term, which is the energy (J) transferred between an air parcel and its environment, dU is the change in internal energy (J) of the parcel, and dW is the work (J) done by or on the parcel. If energy is added to the system then some of it is used to change the internal energy (and temperature) and the rest is used by the parcel of air to do work. Energy is released to the air during condensation of water vapour, deposition of water vapour, freezing of liquid water and energy is removed from the air during melting of ice, sublimation of ice and evaporation of liquid water.

To derive the rate of temperature change Eq. (4.1.17) can be re-written as:

$$dQ = C_V dT + P d\alpha; \tag{4.1.18}$$

where α is the volume element of the parcel

$$dQ = C_V dT + d(P\alpha) - \alpha dP; \tag{4.1.19}$$

Since

$$d(P\alpha) = Pd\alpha + \alpha dP \tag{4.1.20}$$

We obtain

$$dQ = (C_V + R)dT - \alpha dP \tag{4.1.21}$$

Using equation of state (Pα = RT), where R is a universal gas constant and C_V is a specific heat at constant volume

$$dQ = C_P dT - \alpha dP \tag{4.1.22}$$

Therefore,

$$dT = \frac{1}{C_P} dQ + \frac{1}{\rho C_P} dP \tag{4.1.23}$$

By deferentiating Eq. (4.1.23) with respect to time, we arrive at

$$\frac{dT}{dt} = \frac{1}{C_P}\frac{dQ}{dt} + \frac{1}{\rho C_P}\frac{dP}{dt} \tag{4.1.24}$$

or

$$\frac{\partial T}{\partial t} = -u\frac{\partial T}{\partial x} - v\frac{\partial T}{\partial y} - w\frac{\partial T}{\partial z} + \frac{1}{C_P}\frac{dQ}{dt} + \frac{1}{\rho C_P}\frac{dP}{dt} \tag{4.1.25}$$

The heating rate $\frac{dQ}{dt}$ computed from the heating rate due to condensation/evaporation, melting/freezing, sublimation/deposition, and short/long wave radition is given by

$$\frac{dQ}{dt} = \sum \frac{dQ_n}{dt} = \frac{dQ_{c/e}}{dt} + \frac{dQ_{m/f}}{dt} + \frac{dQ_{s/d}}{dt} + \frac{dQ_{sw}}{dt} + \frac{dQ_{lw}}{dt} \tag{4.1.26}$$

The thermodynamic equation can be written in sigma coordinate as follows:

$$\frac{\partial p^\star T}{\partial t} = -m^2\left(\frac{\partial p^\star uT/m}{\partial x} + \frac{\partial p^\star vT/m}{\partial y}\right) - \frac{\partial p^\star T\dot{\sigma}}{\partial \sigma} + \frac{RT_v\omega}{C_{pm}(\sigma + P_t/p_{ast})} + \frac{p^\star Q}{C_{pm}} + F_H T + F_V T, \tag{4.1.27}$$

where c_{pm} is the specific heat for moist air at constant pressure, Q is the diabatic heating, $F_H T$ represents the effect of horizontal diffusion, $F_V T$ represents the effect of vertical mixing and dry convective adjustment, and ω is

$$\omega = p^\star \dot{\sigma} + \sigma \frac{dp^\star}{dt} \tag{4.1.28}$$

where

$$\frac{dp^\star}{dt} = \frac{\partial p^\star}{\partial t} + m(u\frac{\partial p^\star}{\partial x} + v\frac{\partial p^\star}{\partial y}) \tag{4.1.29}$$

The expression for $c_{pm} = c_p(1 + 0.8q_v)$.

4.2 Crop modelling techniques

The impact of climate variability and change on food production has been assessed using a number of methods. Empirical parameterisations of crop yield have been combined with climate modelling and economic modelling (e.g. Iglesias et al., 2000), with the advantage of quantifying impacts in human terms such as levels of risk to hunger (Challinor et al., 2004 and references therein). A disadvantage of this method is that it may introduce errors through the linearisation of crop yield equations (Challinor et al., 2006) and/or the use of monthly data, which does not account for sub-seasonal weather variability (Challinor et al., 2007b, 2005c). Detailed process-based crop models have also been used with climate model output, sometimes scaled down in space. This method can capture the complex biophysical processes associated with climate change that are usually overlooked by empirical studies. However, these models produce results which are location-specific, since the yields depend upon the specific crop variety, soils and management practices used. Whilst this problem can be overcome through the identification of representative farms, this choice can itself be problematic. The problem can also be overcome by applying a bias correction at the output stage (Jagtap and Jones, 2002). Whilst this is a pragmatic approach, some of the benefits of process-based modelling are lost by calibrating outside

the model structure: the coherent simulation of the simulated aspects of crop growth and development is clearly not realistic if a large bias correction is applied to yields.

Process-based crop modelling can also be carried out at the scale of the climate model, providing climate is believed to influence crop yield on that scale (Challinor et al., 2003). The result is a model of intermediate complexity: less complex than location-specific models and more complex than empirical parameterisations. GLAM is a large-area crop model of this sort. This model does not represent the heterogeneity within a climate model grid cell and as a result it has a lower input data requirement than point-based models. Since it is also less complex than many point-based models, the risk of over-parameterisation is reduced (Challinor et al., 2004 and references therein). GLAM contains parameterisations of the mechanisms through which a crop responds to weather and climate. It can, therefore, turn time series of weather into time series of crop yield. Being designed to operate with climate model data in this way is an advantage for a study such as this one. However, this method can omit important fine-scale information on climatic (Baron et al., 2005) and/or non- climatic (Challinor et al., 2004 and references therein) sources of yield variability. Furthermore, there is no evidence of any link at the large scale between yield and non-climatic factors such as management practices, pests and diseases. Hence, this may not be an appropriate scale for the study of non-climatic influences on yield. Despite these issues, large-area crop modelling has shown promising results in current climates in India (Challinor et al., 2004 and references therein) and in other tropical regions (Challinor et al., 2004 and references therein). The crop model used for this study is the general large area model for annual crops (GLAM). GLAM seeks to combine the benifits of empirical modelling (validity over large areas, low input data requirement) with the benifits of process based modelling (capturing the impacts of subseasonal variability and retaining validity under unprecedented conditions, such as are likely under future climates). GLAM is designed for use with daily time series of regional-scale (10-300 Km) weather data, which is usually taken from climate models. Having a daily time step would

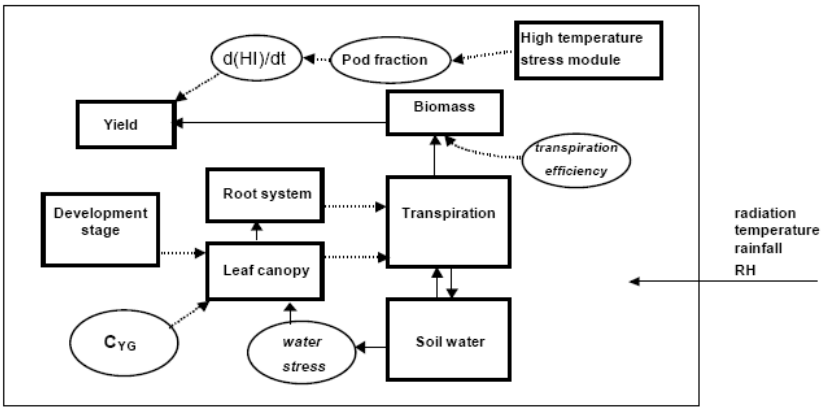

Figure 4.4: GLAM model discription .

allow GLAM to resolve the impacts of sub-seasonal variabilty in weather.

Crop development is determined by accumulating daily mean values of temperature above a base temperature (thermal time) with development stages occuring at specific thermal times. The leaf area index (LAI) is modelled using a maximum growth rate modified by an indicator of water stress. LAI and solar radiation are used to calculate the energy-limited, and will depend on the available water as given by the soil/roots sub model. The ratio of the actual to energy limited evapotranspiration is the indicator of water stress. Use of a transpiration efficiency (which is a function of ambient vapor pressure deficit) then allows the calculation of biomass, which through a harvest index allows the calculation of Yield. GLAM has a soil water balance with 25 layers which simulates evaporation, transpiration and drainage. Separate simulation of biomass accumulation, by use of transpiration efficiency allows specific leaf area (SLA, the mass of leaf per unit area of leaf) to be used as an internal consistency check. Leaf area and leaf mass can be derived independently of each other and can be used to calculate values of SLA which can be compared to typical observed values. Quantitative method to simulate and predict the impacts of high temperature episodes have been included in this model.

The model, as it is used here, uses daily values of solar radiation, minimum and maximum temperature, and rainfall. Radiation is used to determine evapotranspirative demand and

rainfall is used as the input to the upper most soil layer. Maximum and Minimum temperatures are averaged to produce daily mean temperature, and they are also used to calulate the vapour pressure deficit if those data are not available. GLAM has an intelligent sowing window. Sowing occurs on the first day on which the upper most layer is moist enough, or at the end of the window (crisis-sowing) if this does not occur. The soil water model was initialized at the start of the sowing window with zero available soil moisture. Of the impacts on yield due to factors other than weather (pests, diseases, management factors, etc., which act to reduce yields by an amount referred to as the yield gap) only two are modelled explicitly: planting date and soil type. The key soil attribute is the water storage capacity. This is simulated using a lower limit, drained upper limit and saturated limit. Other soil influences are not simulated. All remaining influences on yield are modelled using a single yield gap parameter (YGP), which acts to decrease the leaf area available for transpiration. This allows the model to focus on the impact of weather and climate on the spatio temporal variability of the crop yield. The YGP may also be set to simulate zero yield gap (i.e. yield potential, which is limited only by water, radiation, humidity and temperature). However, it is observed yields with which model output is compared, and this necessiates the calibration of the YGP.

4.2.1 Growth development

The crop is planted either on a specified date, or on the first day that the soil moisture exceeds a given fraction (Csow) of the maximum available soil water. If this threshold is not reached within a given time limit then the crop is planted regardless. Emergence (the first day on which LAI, leaf area index, becomes non-zero) occurs tem (8 has been used for this study) days after sowing. The thermal time elapsed within a given development stage is given by

$$t_{TT} = \int_{t_i}^{T} (T_{eff} - T_b)dt \tag{4.2.1}$$

where t is the time, T_b is the base temperature, below which development ceases, and i is the development stage number, equal to 0 between sowing and flowering, 1 between flowering and pod-filling, 2 between pod-initiation and maximum LAI and 3 between maximum LAI and maturity. Development stage i starts at time t_i and is completed after a specified duration t_{TT} has elapsed and harvest is at maturity.

The effective temperature, T_{eff} is defined as follows using the cardinal temperatures T_b, T_o and T_m, where the subscripts denote base, optimum and maximum temperatures respectively.

$$T_{eff} = \begin{cases} \bar{T} & T_b \leq \bar{T} \leq T_o \\ & T_o - (T_o - T_b)(\frac{(\bar{T} - T_o)}{(T_m - T_o)}) \quad T_o < \bar{T} < T_m \\ T_b & \bar{T} \geq T_m, \bar{T} < T_m \end{cases} \tag{4.2.2}$$

The mean daily temperature, $\bar{T}$ is taken either directly from measurements, or as the average of T_{min} and T_{max}.

The growth of the crop leaf area is determined as follows:

$$\frac{\partial L}{\partial t} = \begin{cases} (\partial L/\partial t)_{max} C_{YG} min(S/S_{cr}, 1) & i<3 \\ 0 & i=3 \end{cases} \tag{4.2.3}$$

where L is the effective LAI, $(\partial L/\partial t)_{max}$ is a prescribed constant and

$$S = \frac{T_T}{T_{T_{pot}}} \tag{4.2.4}$$

is the soil water stress factor, which begins to affect gowth at values less than the critical threshold value S_{cr}. T_T and $T_{T_{pot}}$ are the rates of transpiration and potential transpiration, respectively. C_{YG} is the yield gap parameter, used to reduce LAI from the physical value to an effective value which accounts for the mean effects of pests, diseases and non-optimal management. Yield potential (maximum obtainable yields as determined by weather and crop) may be simulated by setting $C_{YG} = 1$.

The roots grow according to the following equations:

$$\frac{\partial l_v(z=0)}{\partial L} = prescribed{-}constant, V_{EF} = prescribed{-}constant, l_v(z = z_{ef}) = prescribed{-}constant \tag{4.2.5}$$

where l_v is the root length density by volume, z denotes depth into the soil, Z_{ef} is the depth of the root extraction front and V_{EF} is the extraction from velocity. Above-ground biomass (w) is determined by a separate prognostic equation:

$$\frac{\partial W}{\partial t} = T_T min(\frac{E_T}{V}, E_{TN,max}) \tag{4.2.6}$$

where V is the vapour pressure deficit ($VPD = e_{sat}(\bar{T}) - e$, where e is the vapour pressure), E_T is the normalised transpiration efficiency in Pa (i.e. V x $transpiration\ efficiency\ in\ gKg^{-1}$), and $E_{TN,max}$ is the maximum transpiration efficiency in gKg^{-1}. In the case of studies in possible future climates, E_T would be increased from current values as a simulated response to higher CO_2 levels. Where humidity measurements are not used, V is parameterised as

$$V = C_V[e_{sat}(T_{max}) - e_{sat}(T_{min})] \tag{4.2.7}$$

where C_V is a constant (Challinor et al., 2004 and references therein). The saturation vapour pressure deficit at temperature T, $e_{sat}(T)$, is determined (Challinor et al., 2004 and references therein). Yield is determined using harvest index, H_I. For i <2 the yield component is zero, and for $i \geq 2$

$$\frac{\partial H_I}{\partial t} = prescribed - constant \qquad Y = H_I W \tag{4.2.8}$$

4.2.2 Water balance equations

The drained upper limit, lower limit and saturation limit of the soil (θ_{dul}, θ_{ll} and θ_{sat} respectively) are assumed to be constant throughout the profile, which is of depth z_{max} (which is set equal to the maximum attainable rooting depth). The soil is split into N_{SL} soil layers, each with a value of $l_v(z)$ determined by Eq. (4.2.4), and a value of the volumetric soil water content, θ, determined at each time step (1 day) by carrying out the following steps in order: firstly, rainfall runoff occurs according to the US Soil Conservation Service method (Challinor et al., 2004 and references therein):

$$R = \frac{P^2}{(P+S)} \tag{4.2.9}$$

where R is the runoff, P is the precipitation and S is the amount of water that can soak into the soil. The latter is set equal to the saturated hydraulic conductivity of the soil, k_{sat}. Interception by the leaf canopy is ignored since it is a small term made hard to estimate by uncertainty in rainfall data and canopy architecture.

The second step in the soil water balance sequence is drainage, which occurs according to the scheme of Suleiman (1999):

$$\frac{\partial \theta}{\partial t} = -FD(\theta_s - \theta_{dul}) \tag{4.2.10}$$

$$D = C_{d1}\theta_{dul}^2 + C_{d2}\theta_{dul} + C_{d3} \tag{4.2.11}$$

$$F = 1 - \frac{\ln(Q_i + 1)}{\ln(K_{sat} + 1)}, \tag{4.2.12}$$

$$K_{sat} = K_{kS}(\frac{\theta_{sat} - \theta_{dul}}{\theta_{dul}})^2 \tag{4.2.13}$$

where FD is the drainage rate, the factor F accounting for simultaneous inflow from the layer above, θ_s is the initial value of θ, Q_i is the incoming water flux from layer above (P - R in the case of upper most layer). C_{d1}, C_{d2}, C_{d3} and K_{KS} are empirical constants. Finally, water is extracted over the depth z_{ed} by evaporation, and over the root-zone depth by roots, according to the amount of transpiration (See Eqs. (4.2.21) and (4.2.22)). Note that z_{ed} must be a multiple of the soil layer depth (two in the case of the current study). The optimal N_{SL} was found by plotting yield against N_{SL} for a given z_{ed} over a number of environments (not shown). For $N_{SL} > 25$ variation in yield was small (<1), therefore $N_{SL} = 25$ was adopted for all model runs.

4.2.3 Evaporation and transpiration

Transpiration (T_T) and evaporation rates (E) are determined by considering separately the limitations imposed by plants, soil structure, energy availability, and water availability. Potential values of E and T_T are defined as being limited by only the first two of

these constraints. The physiologically limited transpiration is modelled using an empirical relationship based on the data of Azam-Ali(1984):

$$T^p_{T_{pot}} = \begin{cases} T_{T_{max}}(1-\frac{L_{cr}-L}{L_{cr}}) & L<L_{cr} \\ \\ T^p_{T_{pot}}=T_{T_{max}} & L\geq L_{cr} \end{cases} \tag{4.2.14}$$

where L_{cr} is a critical threshold value of L and $T_{T_{max}}$ is the maximum possible potential transpiration rate.

The energy-limited evaporation and transpiration rates (E^e and T^e_T respectively) are defined to be consistent with the Priestley-Taylor equation (Challinor et al., 2004 and references therein) so that potential evapotranspiration rate is given by

$$E^T_{pot} = E^e + T^e_T = \frac{\alpha}{\lambda}\frac{\Delta(R_N - G)}{\Delta + \gamma} \tag{4.2.15}$$

where R_N is the net all-wave radiation, G is the soil heat flux, λ is the latent heat of vapourisation of water, $\Delta = \partial e_{sat}/\partial T$, determined after Bolton (Challinor et al., 2004 and references therein), and γ is the ratio of the specific heat of air at constant pressure to the latent heat of vapourisation of water. The Priestley-Taylor coefficient (α) is parameterised after Jury and Tanner (Challinor et al., 2004 and references therein) as a function of VPD, a constant reference value of VPD (V_{ref}) (Challinor et al., 2004 and references therein) and a pre-correction value $\alpha_o = 1.26$ (Challinor et al., 2004 and references therein):

$$\alpha = 1 + (\alpha_o - 1)\frac{V}{V_{ref}} \tag{4.2.16}$$

This method was chosen because it takes some account of aerodynamic (i.e. advective) effects on the exchange of water vapour from the surface without the need for windspeed data. The net radiation is estimated from the solar radiation using

$$R_N = (1 - A)S_{rad} \tag{4.2.17}$$

where S_{rad} is the incoming short-wave radiation and A is the mean albedo of the surface. This assumes that net long-wave radiation is zero, which is very reasonable under monsoon

(i.e. cloudy) conditions. During monsoon breaks, and during the dry season, clear skies mean that R_N can be over-estimated by up to 100 W m^{-2}. However, sensitivity studies have shown that this has an insignificant effect on the model simulations.

Modelling the light interception using the Beer-Bougert equation (Challinor et al., 2004 and references therein) then gives

$$E^e = (1 - C_G)E^T_{max}e^{-KL} \tag{4.2.18}$$

and

$$T^e_T = E^T_{max}(1 - e^{-KL}) \tag{4.2.19}$$

and where C_G is the constant in the equation for the soil heat flux, $G = C_G R_N e^{-KL}$ (Challinor et al., 2004 and references therein) and k is the extinction coefficient. E^T_{max} , the maximum possible energy-limited evapotranspiration is given by setting G = 0 in Eq. (4.2.14).

The potential (energy and soil-structure limited) daily evaporation is modelled after Cooper (Challinor et al., 2004 and references therein):

$$E^s_{pot} = \frac{E^e}{t_R} \tag{4.2.20}$$

where t_R is the numbers of days since the daily total rainfall was greater than a threshold values of P_{cr}. This threshold value was chosen to be just above zero (1mm) to avoid unrealistically high potential evaporation just after low rainfall.

The potantial (energy and physiology limited) transpiration rate is given by

$$T_{T_{pot}} = min(T^p_{T_{pot}}, T^e_T) \tag{4.2.21}$$

Now that energetic and structural constraints have modelled, it only remains to acount for limited water availability. This is done by partioning the available water according to demand where necessary, so that

$$T_T = T_{T_{pot}} \text{ and } E = E_{pot} \quad for \quad \theta_{pe} \geq E^T_{pot} \text{ ,}$$

$$T_T = \theta_{pe}\frac{T^e_T}{T^e_T + E^e} \tag{4.2.22}$$

and

$$E = \theta_{pe} \frac{E^e}{T_T^e + E^e} \tag{4.2.23}$$

for $\theta_{pe} < E_{pot}^T$

where θ_{pe} is the potentially extractable soil water. This is given by using the parameterisation of passioura (1983 and references therein):

$$\theta_{pe} = \int_0^{Z_{max}} \theta_{cr}(1 - e^{K_{DIF} l_v t_e(z)}) dz \tag{4.2.24}$$

where $t_e(z)$ is the time of first root uptake in layer z, and K_{DIF} is the uptake diffusion coefficient. $t_e(z)$ is determined initially as the time of arrival of the extraction front, and subsequently as the time of arrival of the extraction front, and subsequently as the time at which the equation is re-initiated as a result of wetting such that $\theta(z) > \theta_{cr}$, where

$$\theta_{cr} = \theta_{rll} + C_\theta(\theta_{dul} - \theta_{rll}) \tag{4.2.25}$$

and C_θ is a constant.

4.3 Model calibration

As it is mentioned in the above part of this thesis, GLAM requires daily weather inputs for maximum and minimum temperature, precipitation and solar radiation for corresponding yield years (1996-2007). The yield gap parameter (YGP) takes values between zero and unity, in steps of 0.05, and it is calibrated using observed yields. Hence, calibration is a form of mean bias-correction, which may incorporate the impact of biases additional to the yield gap, such as input data bias and crop model error. GLAM accounts for many processes that are important under climate change. The model contains parameterisations of the impact of changes in atmospheric CO_2 on transpiration efficiency (TE) and SLA, as well as the impacts of mean temperature on crop duration. Subseasonal processes are also parameterised, so that changes in temperature, radiation, atmospheric humidity and

water availability will affect evapotranspiration and crop growth and development. Daily values of VPD, for example, will affect transpiration efficiency. Some processes are not accounted for in this study. The impact of increased ozone concentrations or temperature on transpiration efficiency (as a surrogate for assimilation rates) is not considered. The impact of elevated temperature alone would be to increase transpiration efficiency, whilst the impact of elevated ozone alone would be to decrease transpiration efficiency (Long et al., 2005). In reality these effects interact both with each other and with CO_2 concentrations. Interactions between temperature and elevated CO_2 may or may not be important for crop growth and development. Interactions between water stress, nutrients and CO_2 concentrations are not considered, and neither is any potential downregulation or acclimation to elevated CO_2. Finally, the impact of changes in plant pests and diseases, which has been researched less than impacts on yield, has not been considered in this study. Planting in all simulations referred to in this study occurs on the first day within the planting window on which the available soil moisture exceeds 50% of the maximum.

4.3.1 Dataset

The input climate data for this study is taken directly from the Regional Climate model Simulation. Daily precipitation, mean maximum and minimum temperatures and solar radiation are extracted from the regional climate model output. It has been first simulated for Ethiopia including indian ocean to get a better result then since the study area is the SNNPR region, this region has been taken from the whole domain. Vapour pressure deficit (VPD) was calculated using maximum and minimum temperatures a method which has independently been shown to produce good results (Wang et al, 2004). The cultivated area, production and yield data of SNNPR is collected from Central statistical agency of Ethiopia at zonal/special weredas administrative level from 1995 to 2007 (Since the main rainfall distribution for the selected study area starts in June or July and crops are sown within this month the Meher (crops will be sown in June or July and Harvested in

November/December) yield is taken into account). However, the collection of CSA data is changed with change and expansion of zonal administrative zones/special weredas. For example former North Omo Zone is now classified into three independent administrative zones and two special weredas. But now this administrative zones/special weredas have only about five year independent data. Due to this it is difficult to develop model within current administrative zone/special wereda level. The region is re-divided into 8 zones corresponding to previous common administration, distance and location with respect to each other. Due to lack of yield data for the years mentioned above some of the zones has been jumped, for example, Wolita even if it is not the least wheat producing area, due to unavailability of data it could not be included in this study. The yield data from 1995-2001 has been used for the purpose of calibrating the model while the rest of it is used for the validation of the model. Soil hydrological properties were derived from FAO/UNESCO (1974). The textural categories were used to assign each 0.5^o X 0.5^o grid square to one of seven classes, five ranging in texture from sand to clay, with the addition of lithosol and organic categories. Values of the soil parameters (θ_{sat}, θ_{ll} and θ_{dul}) for each run were obtained by averaging onto the model grid. To account for the uncertainty in the representation of soil hydrological parameters over such large areas using these parameters, three possible sets of the soil parameters were defined, corresponding to mean, upper, and lower values of the maximum available soil water within each of the seven classes. These three sub-classes are referred to as course, medium and fine.

Chapter 5

Results and discussion

5.1 RegCM3 model assessment

In order to assess the performance of RegCM3 in its skill in forecasting rainfall, temperature and other climate variables, it's output is compared to observed value. Central research unit (CRU) has an observed data for rainfall for many years. So RegCM3 output has been compared to CRU data. Since rainfall is the most dominant factor for crop production, only rainfall has been compared for five years data only because CRU data only extends to 2001 GC starting from 1901 GC.

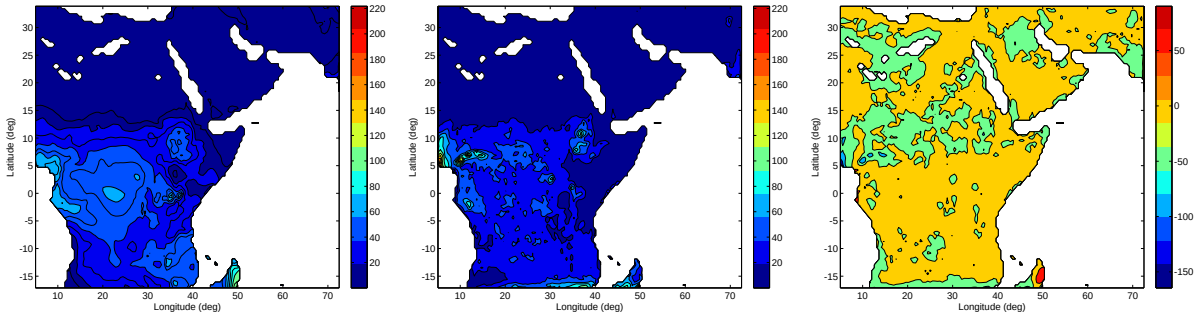

Figure 5.1: Left: Observed rainfall, Middle: Simulated rainfall and Right: Difference of observed and simulated rainfall for 1996.

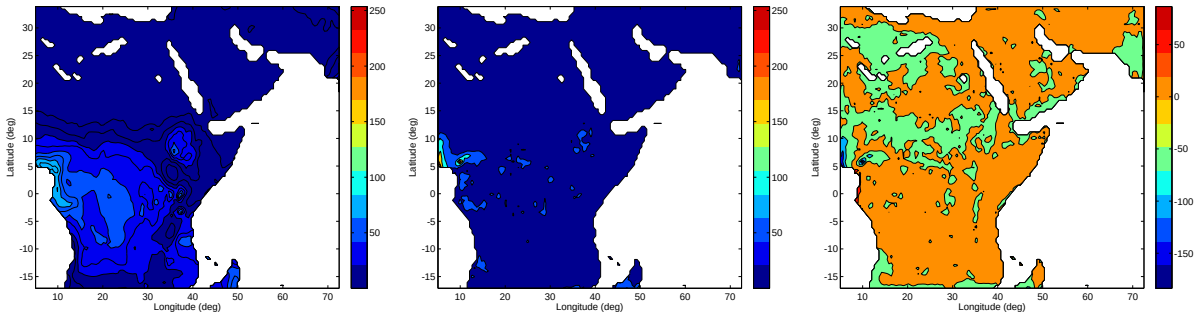

Figure 5.2: Left: Observed rainfall, Middle: Simulated rainfall and Right: Difference of observed and simulated rainfall for 1997.

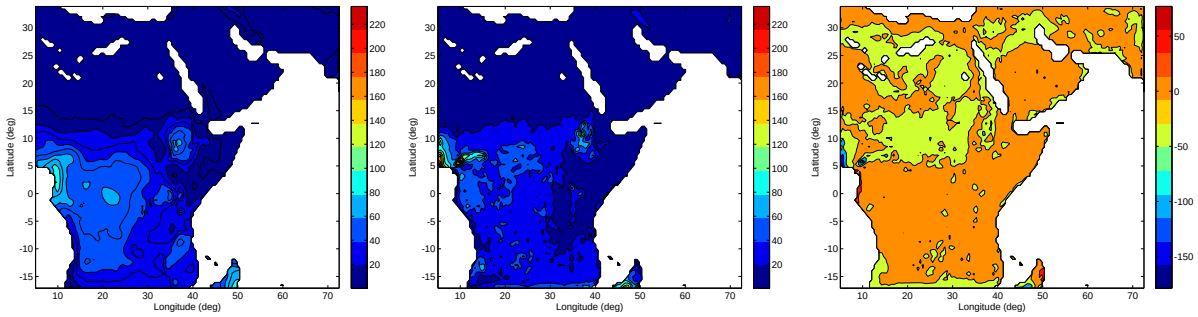

Figure 5.3: Left: Observed rainfall, Middle: Simulated rainfall and Right: Difference of observed and simulated rainfall for 1998.

As it can be seen from the above figure the domain of RegCM3 has almost encompasses Africa and partially Indian Ocean and Atlantic Ocean. Comparing left and middle panel of Figs. 5.1 - 5.6, it can be concluded that RegCM3 precipitation is in good agreement with observation from CRU for the whole domain with a small variation in the central part of Africa and some part of East Africa. The difference of the observed and simulated rainfall shown in the right panel of the figures, depict that almost all the domain shows small discrepancy (yellow colour corresponds to a smaller amount of discrepancy).

However, since the study area for this thesis only focuses on the southern part of Ethiopia, the domain is minimized to see detailed features in the differences shown in the right panel of Figs. 5.1 - 5.6. The reduced domain is shown in Fig. 5.7. The three panels represent 1996, 1997 and 1998 of the differences between simulated RegCM3 and observational CRU precipitation.

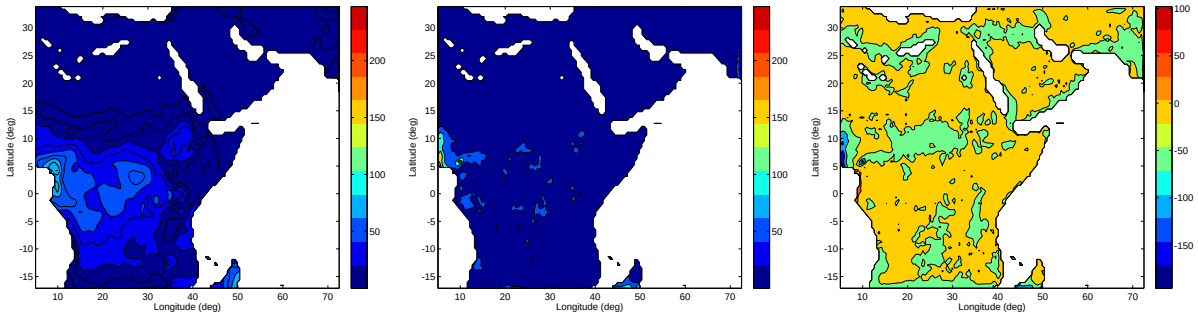

Figure 5.4: Left: Observed rainfall, Middle: Simulated rainfall and Right: Difference of observed and simulated rainfall for 1999.

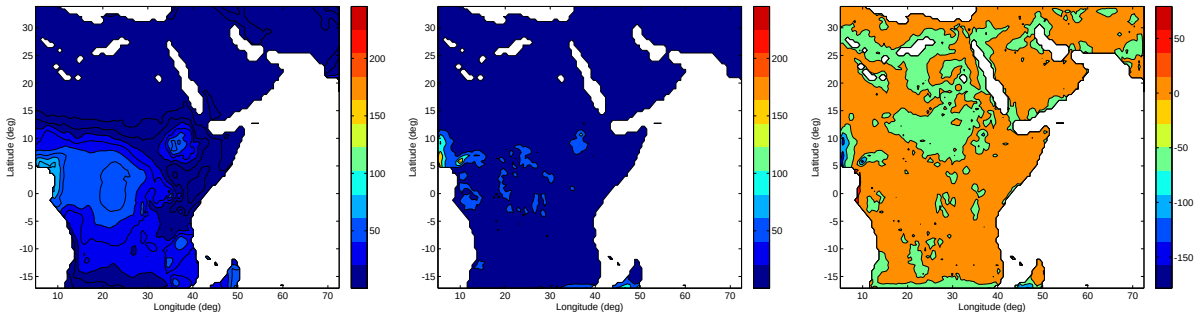

Figure 5.5: Left: Observed rainfall, Middle: Simulated rainfall and Right: Difference of observed and simulated rainfall for 2000.

One can see clearly that RegCM3 simulate relatively high rainfall in highlands area and relatively low rainfall in lowland areas. The difference between simulated RegCM3 and observed CRU precipitation for the remaining 3 years of GLAM simulation (i.e 1999 - 2001) is depicted in the left, middle and right panel of Fig. 5.8 respectively. From both Figs. 5.7 - 5.8, it can be concluded that RegCM3 has low bias over the Southern Ethiopia, simulation domain for GLAM.

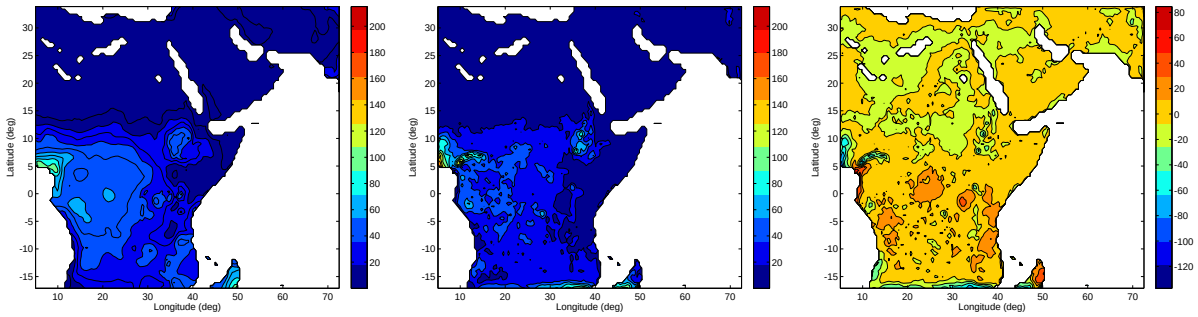

Figure 5.6: Left: Observed rainfall, Middle: Simulated rainfall and Right: Difference of observed and simulated rainfall for 2001.

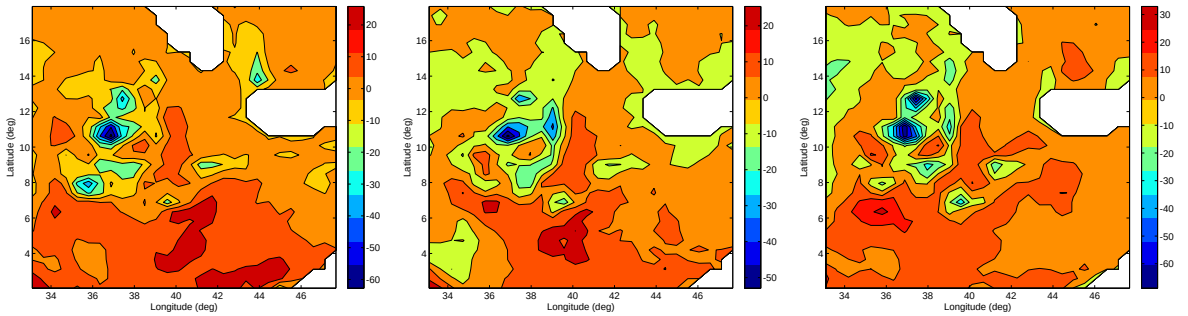

Figure 5.7: Observed minus simulated rainfall difference for Ethiopia domain for the three year periods of time, Left: 1996, Middle:1997 and Right:1998.

5.2 GLAM model assessment

The performance of the model can be evaluated using two methods. The first one is checking the consistency of the model. That is output diagonostic variables from the general large area model such as absorbed radiation, biomass and specific leaf area are determined. The second method for assesing the model is comparing the observed yield with simulated yield time series across the selected regions for different input dataset. For both cases, GLAM validation has used independent (which is not used during calibration part (1996 - 2001)) observed data (2002 - 2007).

The relation ship between simulated yield and rainfall, simulated yield and transpiration and the imapct of using irrigation agricultural system in improving wheat yield production has been assessed.

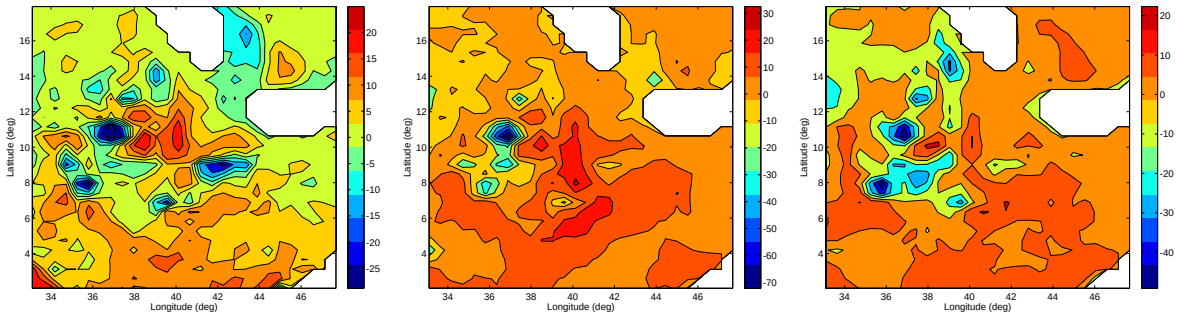

Figure 5.8: Observed minus simulated rainfall difference for Ethiopia domain for the three year periods of time, Left: 1999, Middle:2000 and Right:2001.

5.2.1 Assesment of model internal consistancy

Some tests were carried out on the output from the model for all grid cells in SNNPR using the optimal parameter set. Radiation Use Efficiency (RUE), a concept employed initially in crops research, is a quotient of cumulative biomass to absorbed radiation (Monteith 1972,1977). RUE models have been widely used to estimate productivity over large spatial scales (Gower et al. 1999). Willson (1967) recognized that RUE is reasonably constant for different crops. Monteith (1977) reported a linear relation ship between biomass and absorbed radiation accumulation. The theoretical maximum value for the radiation use efficiency is 2.5 $g(MJ)^{-1}$ when calculated per total radiation absorbed. For well tended C_3 crops (whose carbon-fixation products have three carbon atoms per molecule) the measured RUE is 1.81. Fig. 5.9 and 5.10 depicts the linear relationship between Biomass

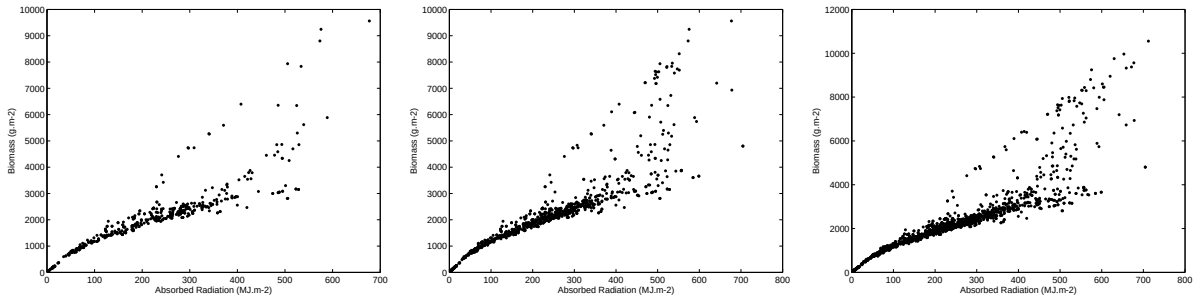

Figure 5.9: End-of-season above-ground biomass vs. cumulative absorbed radiation for the three year periods of time, Left:2002, Middle:2003 and Right:2004.

and Cumulative absorbed radiation from 2002 - 2007. For the period 2002-2007, GLAM

has captured very nicely the linear relation ship between biomass and absorbed radiation as it has been reported by Monteith (1977). However there is increased scattering in the data for cumulative radiation exceeding 400 MJ m^{-2}.

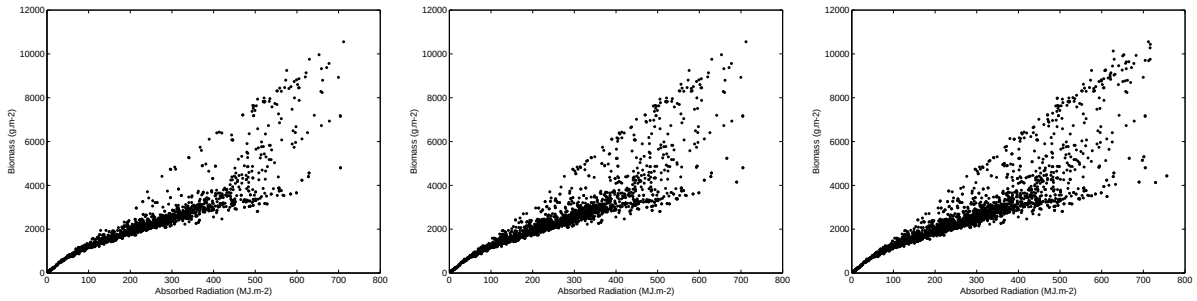

Figure 5.10: End-of-season above-ground biomass vs. cumulative absorbed radiation for the three year periods of time, Left:2005, Middle:2006 and Right:2007.

For 2002, the RUE (the slope of the data) is approximately 2.2 $g(MJ)^{-1}$ which shows a very slight increment from the measured one. For the rest of years the simulated RUE confirms even a slight overestimation which is 2.4 $g(MJ)^{-1}$.

5.2.2 Assesment of model skill

Yield is defined as the production of crop divided by the cultivated land for the production. Its spatial variability is probably related with climatic distribution, soil type and management practices while temporal variability is more related with weather and management practices. As it can be shown from Fig. (5.11), wheat observed yield is

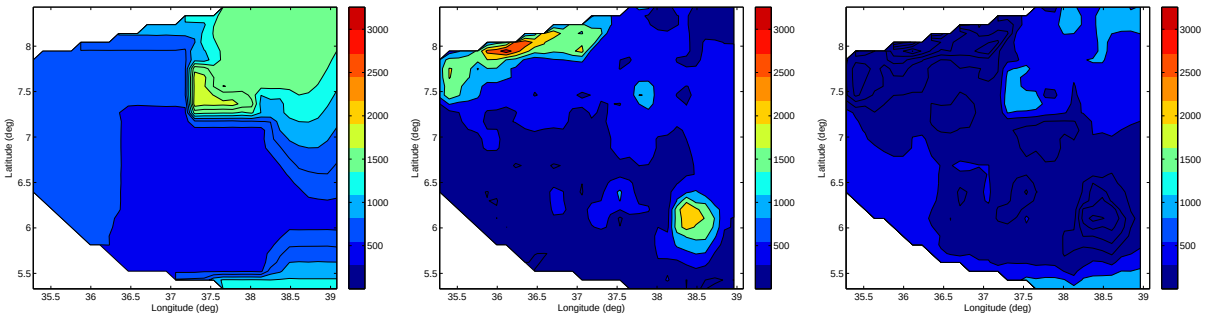

Figure 5.11: Left: Observed yield, Middle: Simulated yield and Right: Difference of observed and simulated yield for 2002.

increasing from south to north. From the simulated yield shown in the middle panel of Fig. 5.11, this trend has been captured very well by the GLAM with the exception of some part of north (some part of keficho-shekicho, Alaba-kembata-tembaro and Hadia) which shows a slight over estimation of yield production. From the right panel (difference of observed and simulated yield) one can clearly notice that, from the dark colour regions, the existence of the correlation of observed and simulated yield (with a yield difference of less than 250 Kg/hectare).

For 2003, the observed yield in most part of SNNPR is almost the same with the exception of the Northern part which includes Gurage, Siltie and Hadia which are highest wheat producing areas. This trend has been captured by GLAM with lower yield production. From Fig. 5.13 of left panel, one can state that some part of North Omo, Burji, Amaro Special Woreda has an enhanced yield production than the Eastern. North-east is still in a superior wheat yield production than the rest of the region. From the right panel of Fig. 5.13 GALM still demonstrates an incredibly good result for the central, North-west and South-east regions.

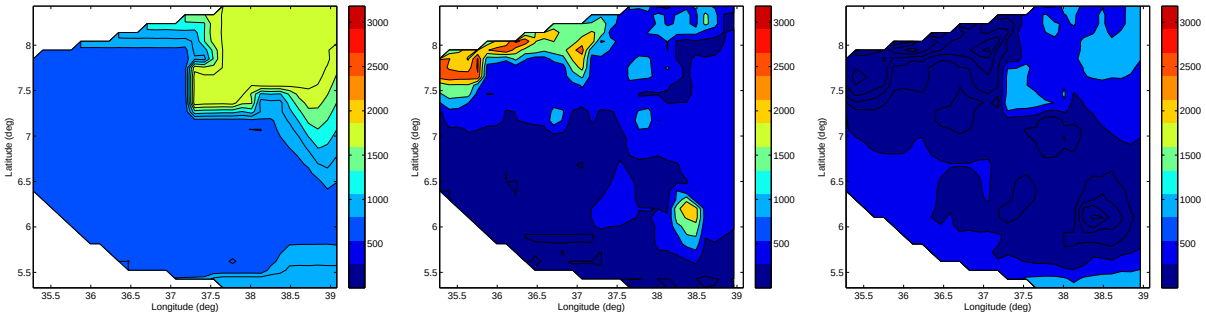

Figure 5.12: Left: Observed yield, Middle: Simulated yield and Right: Difference of observed and simulated yield for 2003.

Figs. 5.14 and 5.15 approve a low correlation of the left and right panel for the North eastern part. One good reason for this could be that, since Gurage, Siltie and Hadia get a better rainfall for the planting season; these regions are an enormous amount of wheat producing areas where as the simulated yield is low due to the a smaller amount rainfall

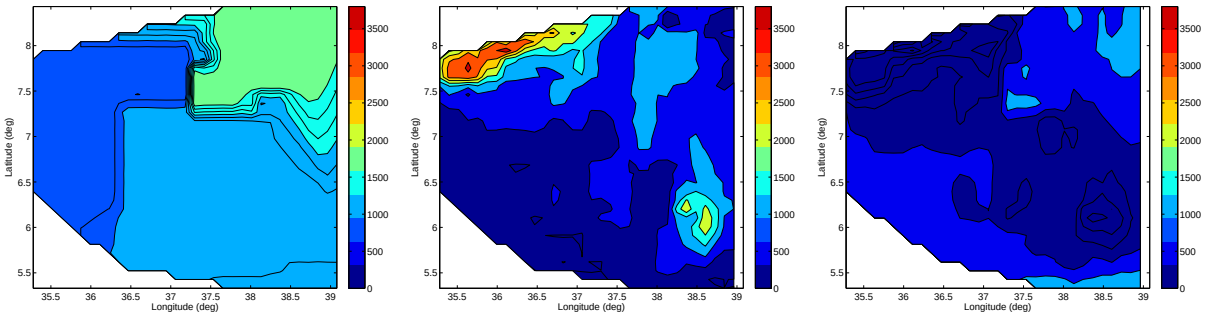

Figure 5.13: Left: Observed yield, Middle: Simulated yield and Right: Difference of observed and simulated yield for 2004.

prediction by the RegCM3. So, the variation of yield for the surveyed and suggested is comparably high than the rest of the regions. The North-east and South-west part

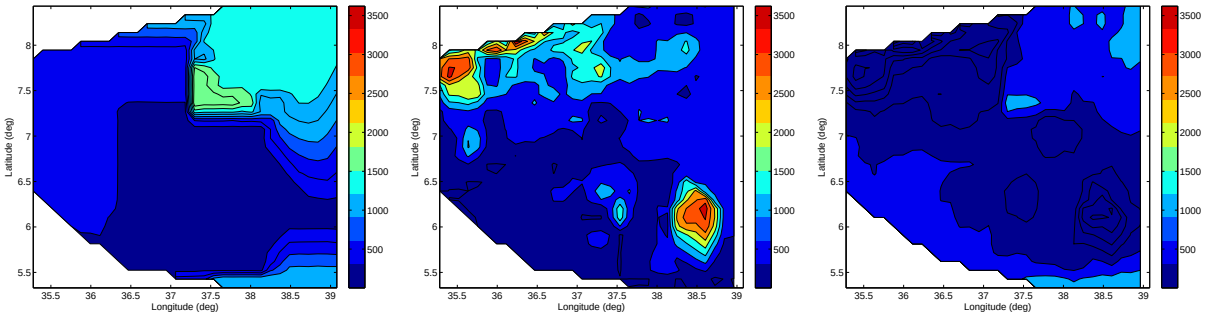

Figure 5.14: Left: Observed yield, Middle: Simulated yield and Right: Difference of observed and simulated yield for 2005.

indicates a lower correlation. This trend roughly continues for the rest of the study years. The mean RMSE varies from 670 Kg/hectar to 920 Kg/hectar over the study years. RMSE for the year 2007 is high compared to the other year's RMSE as shown in Fig. 5.17 of the left panel. This could be due to the deviation of the simualted yield in contrast to observed yield in many zones of the study area. The Bias once more confirms that the low prediction of wheat yield from what has been observed even if the difference is not high. This shows that this difference can be minimized if a better rainfall data has been forcasted.

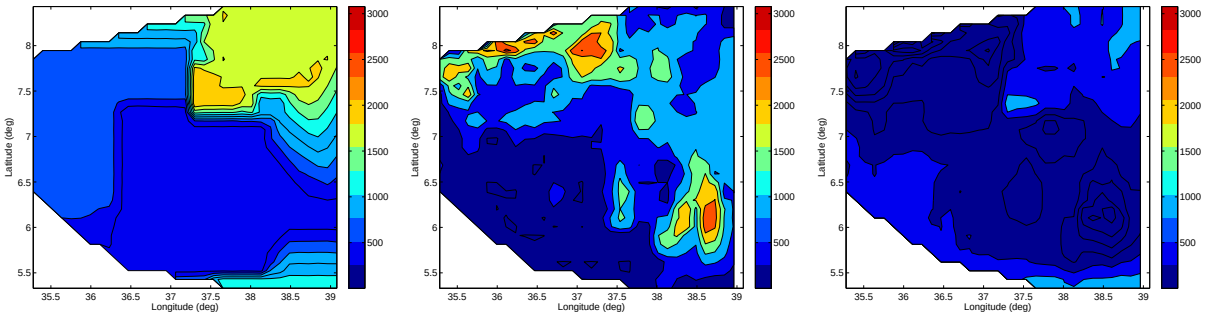

Figure 5.15: Left: Observed yield, Middle: Simulated yield and Right: Difference of observed and simulated yield for 2006 .

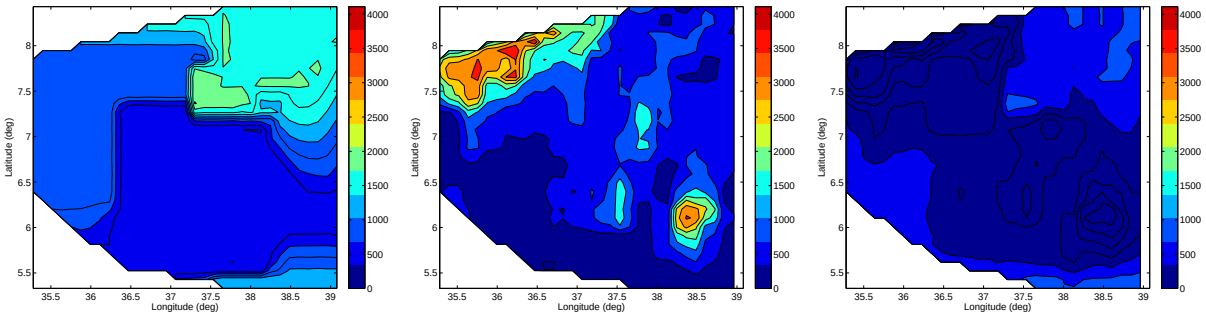

Figure 5.16: Left: Observed yield, Middle: Simulated yield and Right: Difference of observed and simulated Yield for 2007.

5.2.3 Simulated yield and rainfall relationship

Figs. 5.18 and 5.19 convey the simulated response of yield to cumulative rain in SNNPR. From Fig. 5.18 of left panel, it is feasible to notice evidently that the cumulative rainfall amount is low compared to the other panels even if the linear relationship has been achieved. Another interesting point is, this is the year in which low simulated yield has been scored compared to other simulated yield. This is a direct consequence of less rainfall prediction for this year. Figs. 5.18 - 5.19 prove the linear relationship of yield and rainfall which is verified by many researches. Almost for all years, the maximum intensity of rainfall (from Regional Climate Model) ranges between 15 - 45 mm/day which is below the mean annual rainfall received by the region. Middle panel of Fig. 5.18 conveys that there is a better rainfall for the majority of the study region for 2003 than 2002. Right panel of Fig. 5.18 indicates that the cumulative rainfall amount ranges from 20 - 50

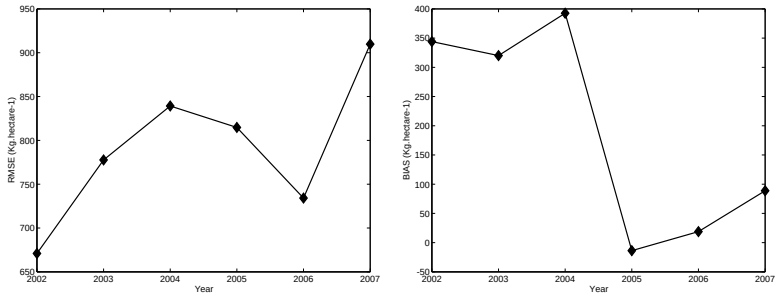

Figure 5.17: Left: RMSE, Right:Bias.

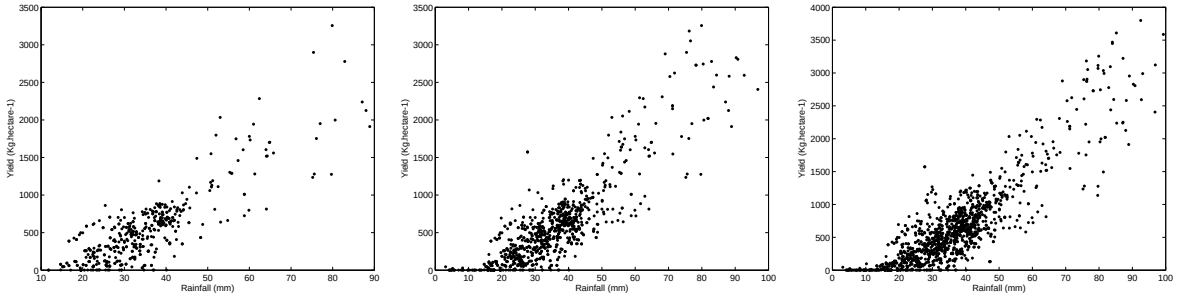

Figure 5.18: Response of simulated yield to rainfall for the three year periods of time, Left:2002, Middle:2003 and Right:2004.

mm/day. The scattered points claim the linear relationship between rainfall and yield. The cumulative rainfall ranges has been changed a little bit for all panels of Fig. 5.19. The yield production has been also enhanced. From the Fig. 5.11 - 5.16 it has been

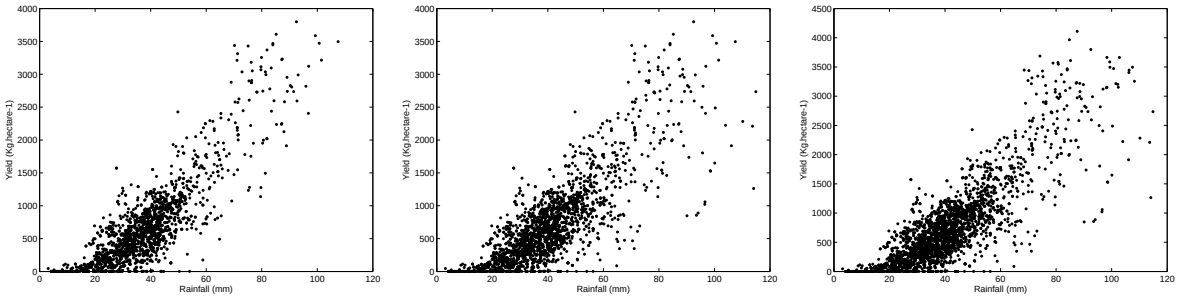

Figure 5.19: Response of simulated yield to rainfall for the three year periods of time, Left:2005, Middle:2006 and Right:2007.

revealed that the simulated yield is lower than the observed yield. So low simulated yield could be the direct influence of low predicted rainfall value.

5.2.4 Simulated yield and transpiration relationship

Transpiration is loss of water from a plant, mainly through the stomata of leaves. Darkness, internal water deficit, and extremes of temperature tend to close stomata and decrease transpiration; illumination, ample water supply, and optimum temperature cause stomata to open and increase transpiration. Crop growth is directly related to transpi-

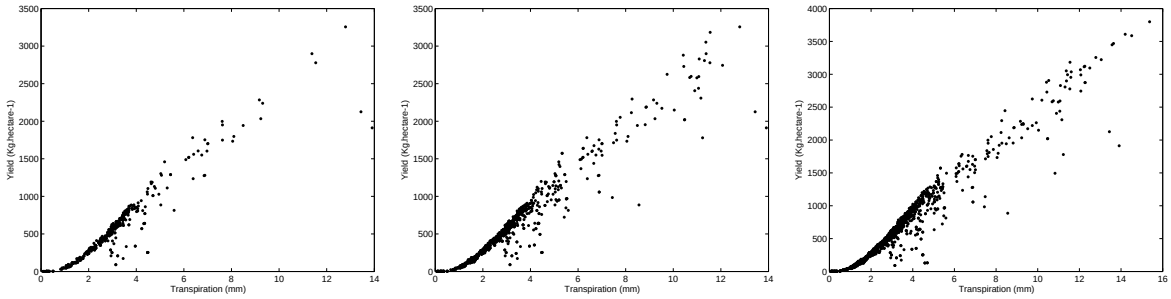

Figure 5.20: Response of simulated yield to transpiration for the three year periods of time, Left:2002, Middle:2003 and Right:2004.

ration. Transpiration is the water that passes through and out of the crop to support the cellular processes that make it grow. The final weight of the crop, or its biomass, is a measure of how efficient the crop was in using water as transpiration for its growth. Researchers have been studying this relationship since the early 19th century, because it is also related to the production of grain needed for food. From the left panel of Fig. 5.20, yield and transpiration has a linear connection. Compared to the other figures, this figure has shown less transpiration concentration. This is a direct consequence of low rainfall observed for this year. The transpiration for the other panels has been improved slightly. The transpiration has been highly concentrated from 1 - 4 mm/day. If the transpiration value is increased, it would directly results in an increased yield production. Compared to Fig. 5.20, Fig. 5.21 has revealed an elevated and denser transpiration. Once again this is as a result of having a higher rainfall for these years than the previous years. The transpiration value ranges from 1 - 7 mm/day.

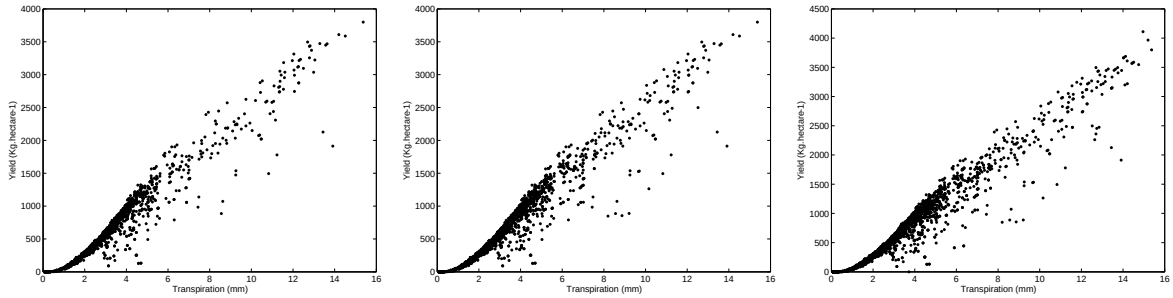

Figure 5.21: Response of simulated yield to transpiration for the three year periods of time, Left:2002, Middle:2003 and Right:2004.

5.2.5 Simulated yield response for irrigational System

So far GLAM has been used for rainfed agricultural system, based on the current Ethiopian agricultural method. In the case of rainfed agriculture plant does not get sufficient amount of water, one reason is due to low rainfall. This could cause plants to experience a water stress. Since water is a main component for plants growth, insufficient amount of water results in low yield production. This reduction in yield due to low rainfall could be

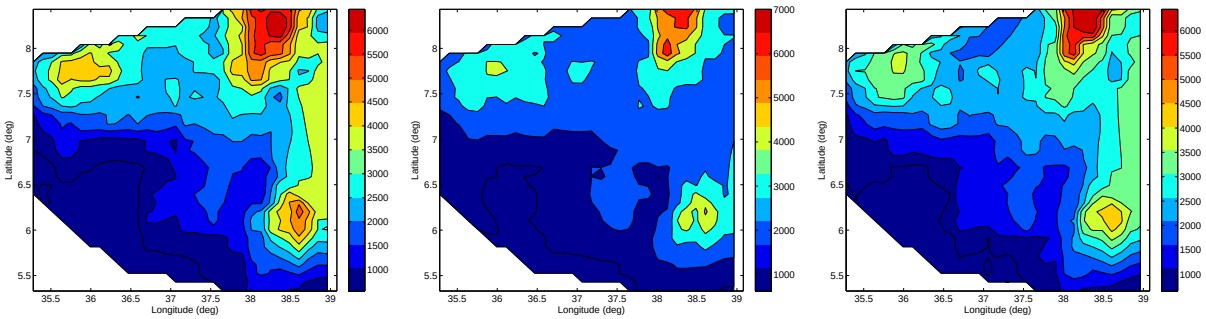

Figure 5.22: Response of simulated yield to irrigational agricultural system for the three year periods of time, Left:2002, Middle:2003 and Right:2004.

avoided if irrigation is used instead of rainfed. As Figs. 5.22 and 5.23 strongly confirm there is a great improvement in wheat yield production for the whole study period in the entire part of the study regions. GLAM has simulated a reduced amount of wheat yield for rainfed agricultural system contrasted to surveyed yield. This is not as a result of the tendency of low estimation of yield by the model. But, since rainfall is the main component which determines the availability of water content in the soil, so a reduction

of rainfall could cause the plant to wilt. This constraint can be avoided if the system is irrigation. Figs. 5.22 and 5.23 verify this. As it can be viewed from Figs. 5.22 and 5.23, the least wheat yield production areas, which lies in the South-western part, has given a yield of 1000 Kg/hectare upon use of irrigation. The central part as well as the Northern has shown high yield for non water stress agricultural system.

It can be seen without doubt the loss in yield production by comparing Figs. 5.11 - 5.16 and Figs. 5.22 - 5.23. Another point that can be taken out from irrigation simulation

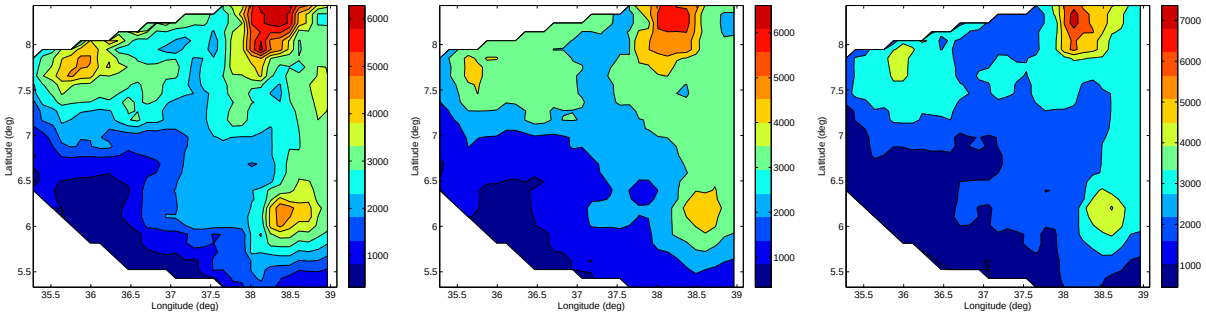

Figure 5.23: Response of simulated yield to irrigational agricultural system for the three year periods of time, Left:2005, Middle:2006 and Right:2007.

is the confirmation of how much rainfall quantity affects yield. Low simulated yield has been observed for rainfed system compared to irrigation because RegCM3 has predicted less rainfall amount. So GLAM could give a magnificent result if the RegCM3 output has been corrected (calibrated).

Chapter 6

Conclusion

The general large-area model (GLAM) for annual crops has been used for wheat prediction in SNNPR. The model is relatively simple, having 40 parameters, 5 of which vary spatially (3 soils parameters, planting date, and the yield gap parameter), 20 of which are crop-specific.

The regional climate model (RegCM3) has been used to generate climate variables. Climate variables generated by RegCM3 for use in GLAM are precipitation, solar radiation, minimum and maximum temperature. Since precipitation is one of major climate variables that strongly influence GLAM yield forcast, we compared RegCM3 precipitation with observed precipitation from CRU dataset. RegCM3 precipitation has generally a positive bias over highlands and a negative bias over lowlands of Ethiopia. The RegCM3 precipitation over SNNPR is negatively biased in general.

All the internal consistency checks that are used to ensure the performance of the crop model prove that GLAM performs magnificently. The radiation use efficiency (RUE) of the computed value is comparable to the measured one. The relationship between rainfall and yield is linear as expected. The relationship between biomass and absorbed radiation is also found to be linear. This is in agreement with results reported in Monteith (1977). GLAM simulated yield output has been shown to have a high correlation with the observed yield in most of central part of the study area. GLAM yield, however, has a slight low-correllation with the observed yield in the North-east and South-west part of the

study area. One of the main cause of the low-correlation of the observed and simulated yield and a high RMSE for some of the years could be the negative bias in precipitation data that has been used.

GLAM yield values are negatively biased in general. This is anticipated since RegCM3 simulation underestimates precipitation over most parts of SNNPR region of Ethiopia. This might introduce water stress in the model. To verify the presence of water stress in the model, we have swithced the model from rainfed to irrigation. GLAM simulations in irrigation mode have resulted in yield which exceeds observed yield indicating water stress in rainfed case. Therefore, direct use of RegCM3 output as an input could give us unpleasant result. It could be advisable to bias correct at least the precipitation in order to match with the observed precipitation. Another constraint that could prevent from not getting a good result from GLAM is lack of the availability of yield data. GLAM estimate very nicely if a long term ($>$ 15 years) yield data is available. This is possible since we can calibrate GLAM over a longer period.

In conclusion, we have found that the GLAM performance is quite good for wheat yield prediction over SNNPR region of Ethiopia. The negative yield bias is related to inappropriate rainfall inputs to the model. Our next task should be directed at getting rainfall calibrated and run the GLAM model to confirm what we observed in this study.

Bibliography

1. Azam-Ali, S.N., 1984. Environmental and physiological control of transpiration by groundnut crops. Agric. For. Meteorol. 33,129-140.
2. Baron, C., Sultan, B., Balme, M., Sarr, B., Teaore, S., Lebel, T., Janicot, S., Dingkuh, M., 2005. From GCM grid cell to agricultural plot:scale issues affecting modelling of climate impacts. Phil. Trans. R. Soc. 1463 (360), 2095-2108.
3. Batts, G.R., Morison, J.I.L., Ellis, R.H., Hadley, P., Wheeler, T.R., 1997. Effects of CO2 and temperature on growth and yield of crops of winter wheat over four seasons. Eur. J. Agron. 7,43-52.
4. Challinor, A.J., Wheeler, T.R., Craufurd, P.Q., Slingo, J.M., Grimes, D.I.F., 2004. Design and optimisation of a large-area process-based model for annual crops. Agric. For. Meteorol. 124, 99-120.
5. Challinor, A.J., Slingo, J.M., Wheeler, T.R., Doblas-Reyes, F.J., 2005. Probabilistic simulations of crop yield over western India using the DEMETER seasonal hindcast ensembles. Tellus A 57, 498-512.
6. Challinor, A.J., Wheeler, T.R., Osborne, T.M., Slingo, J.M., 2006. Assessing the vulnerability of crop productivity to climate change thresholds using an integrated crop-climate model.In: Schellnhuber, J., Cramer, W., Nakicenovic, N., Yohe, G., Wigley, T.M.L. (Eds.), Avoiding Dangerous Climate Change. Cambridge University Press,pp. 187-194.
7. Challinor, A.J., Slingo, J.M.,Wheeler, T.R., Craufurd, P.Q.,Grimes, D.I.F., 2003. Towards a combined Seasonal weather and crop productivity forcasting system:dterm -ination of the spatial correlation scale. J. Appl. Meteorol.
8. Chee-Kiat, T., 2006. Application of satellite-based rainfall estimates to crop yield

forecasting in Africa. Ph.D. thesis, University of Reading.

9. Cox, G.M., Gibbons, J.M., Wood, A.T.A., Craigon, J., Ramsden, S.J., Crout, N.M.J., 2006. Towards the systematic simplification of mechanistic models. Ecol. Model. 198 (12), 240-246.
10. Doorenbos, J., Kassam, A.H., 1979. Yield Response to Water. FAO Irrigation and Drainage 33, FAO, Viale delle Terme diCaracalla, 00100 Rome, Italy.
11. Downing, T.E. (Ed.), 1996. Climate change and world food security. NATO ASI Series. Series I: Global Environmental Change 37, Springer, Berlin, 662 pp.
12. Easterling, W.E., 1996. Adapting North-American agriculture to climate change in review. Agric. For. Meteorol. 80 (1), 153.
13. FAO/UNESCO, 1974. FAO/UNESCO Soil Map of the World, 1:5,000,000, ten vol umes.
14. Garcia-Huidobro, J., Monteith, J.L., Squire, G.R., 1982. Time, temperature and germination of pearl millet (Pennisetum typhoides). I.Constant temperature. J. Exp. Bot. 33, 288-296.
15. Goudriaan, J., Unsworth, M.H., 1990. Implications of increasing carbon dioxide and climate change for agricultural productivity and water resources. In: Kimball, B.A., Rosenberg, N.J., Allen, L.H. (Eds.), Impact of Carbon Dioxide, Trace Gases, and Climate Change on Global Agriculture. Special Publication No. 53. American Society of Agronomy, Madison, WI, pp. 111-130.
16. Hadley, P., Roberts, E.H., Summerfield, R.J., Minchin, F.R., 1983. A quantita tive model of reproductive development in cowpea (Vigna unguiculata (L.) Walp.) in relation to photoperiod and temperature, and implications for screening germplasm. Ann.Bot. 51, 531-543.
17. Hansen, J.W., Jones, J.W., 2000. Scaling-up crop models for climatic variability applications. Agric. Syst. 65, 43-72.
18. Hammer, G.L., Sinclair, T.R., Boote, K.J., Wright, G.C., Meinke, H., Bell, M.J., 1995. A peanut simulation model. I. Model development and testing. Agron.J.87, 1085-1093.
19. Harrison, P., Butterfield, R., Downing, T. (Eds.), 1995. Climate change and agri culture in Europe assessment of impacts and adaptation. University of Oxford, UK,

411 pp.

20. Holton, J.R., An Introduction To Dynamic Metrology. Fourth Edition.
21. Hunt, R., 1990. Basic Growth Analysis: Plant Growth Analysis for Beginners. Unwin Hyman, London, p. 38.
22. Iglesias,A., Rosenzweig,C.,Persia, D.,2000. Agricultural impacts of climate change in spain: developing tools for a spatial analysis. Global Environment Change-Human and Policy Dimensions 10(1),69-80.
23. Ingige, 2000. Drought-prone in tropical regions. p.78.
24. IPCC, 2001. Climate Change 2001: Impacts, Adaptation, and Vulnerability. Contri bution of Working Group II to the Third Assessment Report of the Intergovernmental Panel on Climate Change, Cambridge University Press, p. 255.
25. Jacobson, M.Z., Fundamentals of Atmospheric Modeling. Second Edition.
26. Jagtap, S.S., Jones, J.W., 2002. Adaptation and evaluation of the CROPGRO-soybean model to predict regional yield and production. Agric. Ecosyst. Environ. 93, 73-85.
27. Kakani, V.G., 2001. Quantifying the Effects of High Temperature and Water Stress in Groundnut. PhD Thesis. University of Reading, U.K.
28. Kimball, B.A., Kobayashi, K., Bindi, M., 2002. Responses of agricultural crops to free-air CO2 enrichment. Adv. Agron. 77, 293-368.
29. Landau, S., Mitchell, R.A.C., Barnett, V., Colls, J.J., Craigon, J., Payne,R.W., 2000. A parsimonious, multiple-regression model of wheat yield response to environment. Agric.For. Meteorol. 101, 151-166.
30. Long, S.P., Ainsworth, E.A., Rogers, A., Ort, D.R., 2004. Rising atmospheric carbon dioxide: plants FACE the future. Annu. Rev. Plant Biol. 55, 591-628.
31. Long, S.P., Ainsworth, E.A., Leakey, A., Morgan, P.B., 2005. Global food insecurity. Treatment of major food crops to elevated carbon dioxide and ozone under large-scale fully open-air conditions suggest models may seriously over-estimate future yields. Phil. Trans. R. Soc. 1463 (360), 2011-2020.
32. Monteith JL. 1977. Climate and the efficiency of crop production in Britain. Series B 281: 277-294.
33. Morison, J., 1998. Stomatal responses to increased CO2 concentration. J. Exp. Bot.

49, 443-452.

34. Morison, J.I.L., Lawlor, D.W., 1999. Interactions between increasing CO2 concentra tion and temperature on plant growth. Plant Cell Environ. 22, 659-682.

35. Nastasi, J.C, 1994. High potential wheat producing areas in Ethiopia. J. Ser. Fer 78, 25-29.

36. Parry, M.L., Rosenzweig, C., Iglesias, A., Livermore, M., Fischer, G., 2004. Effects of climate change on global food production under SRES emissions and socio-economic scenarios. Global Environmental Change Human and Policy Dimensions 14 (1),53 -67.

37. Peiris, D.R., Crawford, J.W., Grashoff, C., Jefferies, R.A., Porter, J.R., Marshall, B., 1996. A simulation study of crop growth and development under climate change. Agric. For. Meteorol. 79, 271-287.

38. Porter, J.R., Gawith, M., 1999. Temperatures and the growth and development of wheat: a review. Eur. J. Agron. 10, 23-36.

39. Rosenzweig, C., Allen, L., Harper, L., Hollinger, S., Jones, J.(Eds.), 1995. Climate Change and Agriculture: Analysis of Potential International Impacts. American So ciety of Agronomy, Vol. 59, 382 pp.

40. Slafer, G.A., Rawson, H.M., 1994. Sensitivity of wheat-phasic development to major environmental factors: a re-examination of assumptions made by physiologists and modellers. Aust. J.Plant Physiol. 21, 393-426.

41. Smith, J.B., 1997. Setting priorities for adapting to climate change. Global Environ. Change Hum. Policy Dimensions 7 (3), 251-264.

42. Srinivasan, A., Takeda, H., Senboku, T., 1996. Heat tolerance in food legumes as evaluated by cell membrane thermostability and chlorophyll flourescence techniques. Euphytica 88, 35-45.

43. Suleiman, A.A., 1999. Assessing and modeling the spatial variability of soil water redistribution and wheat yield along a sloping landscape. Ph.D. Thesis.Crop and Soil Sciences Department, Michigan State University.

44. Wang, E., Robertson, M.J., Hammer, G.L., Carberry, P.S.,Holzworth, D., Meinke, H., Chapman, S.C., Chapman, J.N.G.,Hargreaves, J.N.G., Huth, N.I., McLean, G. , 2002. Development of a generic crop model template in the cropping system model

APSIM. Eur. J. Agron. 18,121-140.

45. Winter and Musick, 1993. Optimum planting date and its impacts on crop yield production. p. 23-29.
46. Wheeler, T.R., Craufurd, P.Q., Ellis, R.H., Porter, J.R., Prasad, P.V.V.,2000.variability and the annual yield of crops.Agric.Ecosyst.Environ.Temperature 82,159-167.
47. Wheeler, T.R., Batts, G.R., Ellis, R.H., Hadley, P., Morison, J.I.L., 1996a. Growth and yield of winter wheat (Triticum aestivum) crops in response to CO2 and temper ature. J. Agric. Sci. 127, 37-48.
48. Wheeler, T.R., Batts, G.R., Ellis, R.H., Hadley, P., Morison, J.I.L., 1996a. Growth and yield of winter wheat (Triticum aestivum) crops in response to CO2 and temper ature. J. Agric. Sci. 127, 3748.
49. Wolf, J., Van Diepen, C.A., 1995. Effects of climate change on grain maize yield potential in the European Community. Climatic Change 29 (3), 299331.

Declaration

This thesis is my original work, has not been presented for a degree in any other University and that all the sources of material used for the thesis have been dully acknowledged.

Name: Jemal A.

Signature:

Place and time of submission: Addis Ababa University, July 2010

This thesis has been submitted for examination with my approval as University advisor.

Name: Dr.Gizaw M.

Signature: